Published in final edited form as:
Epilepsia. 2007 November ; 48(11): 2023–2046. doi:10.1111/j.1528-1167.2007.01189.x.

Structural Consequences of *Kcna1* Gene Deletion and Transfer in the Mouse Hippocampus

H. Jürgen Wenzel[1], **Helene Vacher**[2], **Eliana Clark**[2], **James S. Trimmer**[2], **Angela L. Lee**[3], **Robert M. Sapolsky**[3], **Bruce L Tempel**[4], and **Philip A. Schwartzkroin**[1]

[1]Department of Neurological Surgery, School of Medicine, University of California, Davis, CA

[2]Department of Pharmacology, School of Medicine, University of California, Davis, CA

[3]Department of Biological Sciences, Stanford University, Stanford, CA

[4]Departments of Otolaryngology and Pharmacology, School of Medicine, University of Washington, Seattle, WA

Abstract

Purpose—Mice lacking the Kv1.1 potassium channel α subunit encoded by the *Kcna1* gene develop recurrent behavioral seizures early in life. We examined the neuropathological consequences of seizure activity in the Kv1.1$^{-/-}$ ("knock-out") mouse, and explored the effects of injecting a viral vector carrying the deleted *Kcna1* gene into hippocampal neurons.

Methods—Morphological techniques were used to assess neuropathological patterns in hippocampus of Kv1.1$^{-/-}$ animals. Immunohistochemical and biochemical techniques were used to monitor ion channel expression in Kv1.1$^{-/-}$ brain. Both wild-type and knockout mice were injected (bilaterally into hippocampus) with an HSV1 amplicon vector that contained the rat *Kcna1* subunit gene and/or the *E.coli lacZ* reporter gene. Vector-injected mice were were examined to determine the extent of neuronal infection.

Results—Video/EEG monitoring confirmed interictal abnormalities and seizure occurrence in Kv1.1$^{-/-}$ mice. Neuropathological assessment suggested that hippocampal damage (silver stain) and reorganization (Timm stain) occurred only after animals had exhibited severe prolonged seizures (status epilepticus). Ablation of *Kcna1* did not result in compensatory changes in expression levels of other related ion channel subunits. Vector injection resulted in infection primarily of granule cells in hippocampus, but the number of infected neurons was quite variable across subjects. Kcna1 immunocytochemistry showed "ectopic" Kv1.1 α channel subunit expression.

Conclusions—*Kcna1* deletion in mice results in a seizure disorder that resembles – electrographically and neuropathologically – the patterns seen in rodent models of temporal lobe epilepsy. HSV1 vector-mediated gene transfer into hippocampus yielded variable neuronal infection

Keywords

Epilepsy; Gene therapy; Hippocampal pathology; Knock-out; Potassium channel; Seizures

Correspondence to: Philip A. Schwartzkroin, PhD Department of Neurological Surgery University of California, Davis School of Medicine- Neuroscience Building, Room 612G 1515 Newton Court Davis, CA, 95618 Phone: (530)-754-5029 Fax: (530) 754-8976 paschwartzkroin@ucdavis.edu.

Introduction

In the past decade, mutations in over 70 genes have been identified and linked to inherited epilepsies (e.g., Noebels, 2003). Further, studies of epilepsy-related genes in animal models have provided important insights into potential underlying mechanisms (Burgess, 2006; Noebels, 2006). For example, changes in gene expression that give rise to up- or down-regulation of receptors/transmitters can affect seizure frequency and/or alter seizure threshold (e.g., Baraban et al., 1997; Mazarati et al., 2000; Richichi et al., 2004). These genetic and molecular insights into seizure propensity have been supplemented by the discovery of a large number of single gene mutations - in mice and in man - that appear to determine chronic seizure disorders (Burgess and Noebels, 1999; Steinlein and Noebels, 2000; Yang and Frankel, 2004). In particular, mutations and/or deletions of genes regulating the expression of key ion channels – e.g., potassium channels – can result in enhanced or impaired channel function (i.e., channelopathies) (Mulley et al., 2003; Burgess, 2006; Noebels, 2006).

Voltage-gated potassium channels (Kv channels) are critical regulators of neuronal excitability, and mutations in potassium channel subunit genes are associated with diverse clinical phenotypes including seizure disorders (Noebels, 2003). Voltage-gated potassium channels are membrane protein complexes of four pore-forming and voltage-sensitive α subunits and up to four cytoplasmatic subunits (Trimmer, 1998). The Kv1.1 α subunit (the product of the *Kcna1* gene) was the first mammalian Kv channel subunit to be cloned (Tempel et al., 1988). In both rodent and human brain, it is abundantly and widely expressed (Tempel et al., 1988; Wang et al. 1993, 1994; Rhodes et al., 1995; Coleman et al., 1999; Trimmer and Rhodes, 2004). Expression of Kv1.1α subunits in heterologous cells results in formation of homotetrameric channels, mediating a delayed rectifier potassium current (Stuhmer et al., 1988). However, in native cells, Kv1.1 exists exclusively in heteromeric channels containing Kv1.2 and Kv1.4 α subunits and Kvβ1 and Kvβ2 auxiliary subunits (Koch et al., 1997; Shamotienko et al., 1997). Previous studies have shown that Kv1.1-containing potassium channels are predominantly localized to axons (juxta-paranodal regions of myelinated axons and fine non-myelinated axons) and axon terminals in hippocampus (Wang et al., 1993, 1994; Rhodes et al., 1995, 1997; Monaghan et al., 2001) and cerebellum (Wang et al., 1993; Rhodes et al., 1997; Strassle et al., 2005). The co-assembly of Kv1.1 with Kv1.4 (Ruppersberg et al., 1990) and/or Kvβ subunits (Rettig et al., 1994) in heterologous cells gives rise to channel properties distinct from those channels composed of Kv1.1 alone (A-current vs. delayed rectifier). Furthermore, the subunit composition of Kv1.1-containing channels can affect intracellular trafficking and surface expression efficiency; Kv1.1 homotetramers are predominatly retained intracellularly, while Kv1.1-containing heterotetramers are expressed on the cell surface (Manganas & Trimmer, 2000).

Previous reports from our laboratory have described the functional consequences of the mouse *Kcna1* gene deletion (Smart et al., 1998; Rho et al., 1999; Lopantsev et al., 2003). Deletion of the *Kcna1* gene resulted in Kv1.1 knock-out mice which exhibit frequent recurrent spontaneous seizures, beginning 2-4 weeks postnatally, consistent with the expected developmental expression of Kcna1 (Smart, et al., 1998; Grosse et al., 2000; Hallows and Tempel, 1998; Trimmer, unpublished). Seizures in Kv1.1$^{-/-}$ mice display many of the characteristics of temporal lobe seizures in other rodent models of temporal lobe epilepsy (e.g., initial “freezing,” then sniffing and licking, rearing, and progressing through forelimb clonus and generalized tonic-clonic seizures), suggesting that limbic structures - e.g., the hippocampus - may play an important role in the epileptic process (Rho et al., 1999). Kv1.1 knock-out mice also have reduced evoked seizure thresholds, as well as abnormal action potential conduction in peripheral nerves (Smart et al., 1998; Rho et al., 1999). Analogously, neuronal excitability is increased dramatically in neurons of the medial nucleus of the trapezoid body of Kv1.1$^{-/-}$ mice, caused by a decrease in the low-voltage activated current I_{KL}, to which the Kv1.1 subunits

normally contribute (Brew et al., 2003), limiting both spike frequency and jitter (Gittelman & Tempel, 2006).

The identification of disease-causing gene mutations and the development of genetic models closely replicating human CNS pathologies have not only increased our understanding of underlying molecular/genetic events, but also opened new opportunities for therapeutic interventions of a variety of diseases via gene transfer (reviewed in Vadolas et al., 2002; Verma and Weitzman, 2005) -- e.g., cancers and diabetes (Kaminski et al., 2002; Welsh, 1999) and neurodegenerative disorders (McCown, 2004, 2005; Glorioso and Fink, 2004; Chen et al., 2005; Deglon and Hantraye, 2005; Frampton et al., 2005). Only a small number of epilepsy studies have been carried out to examine the potential of gene transfer techniques for inducing the expression of "therapeutic molecules" that might modulate or influence brain excitability (e.g., see Fisher and Ho, 2002; Lin et al., 2003; Vezzani, 2004; McCown et al., 2004; Richichi et al. 2004). We have begun to pursue that strategy within the context of seizure activity in Kv1.1 knockout mice, focusing on Kv1.1 α subunit replacement via gene transfer into critical subpopulations of hippocampal neurons. While there are many potential strategies for testing the potential of gene transfer approaches, we've chosen to focus on replacing a gene product known to be deficient in this model, the absence of which is central to the epileptic phenotype.

The goals of the present study were: (1) to expand our understanding of seizure-related pathologic features of the Kv1.1 knock-out mouse model, particularly as they relate to seizure occurrence; (2) to localize, ultrastructurally, Kv1.1 channels in wildtype hippocampal neurons and axons of major hippocampal pathways; (3) to determine the nature and extent of compensatory changes in the expression and localization of related ion channels in the Kv1.1 knock-out mouse; and (4) to determine the structural expression pattern of Kcna1 following *Kcna1* gene transfer into hippocampus of mice lacking *Kcna1*.

Materials and Methods

Animals

The morphological analyses of Kcna1 localization, gene deletion and viral vector-associated gene transfer into hippocampal neurons were carried out in brains of homozygous Kv1.1 knock-out mice of the *Kcna1*^{tm1Tem} strain (total n=64). The *Kcna1* gene deletion was generated on a 129Sv genetic background. Description of the gene deletion protocol and initial characterization of these mice have been published (Wang et al., 1994; Smart et al., 1998). Kv1.1 knock-out features were compared with those of wild-type mice of the same background and age (total n=56). The majority of investigations were carried out on 2-5 month old mice; a small number of older animals (10-12 months) were also included for comparison. All experiments were conducted in compliance with the NIH Guide for Care and Use of Laboratory Animals, and were approved by the Institutional Animal Care Committee of the University of California at Davis.

Video/EEG Monitoring

Both wild-type and Kv1.1$^{-/-}$ mice were prepared for video/EEG monitoring. Recordings were carried out with a Telefactor video/EEG system (Telefactor, W. Conshohocken, PA). Chronic EEG electrodes were surgically implanted (ketamine/xylazine anesthesia) using sterile technique. Micro-screws (stainless steel) served as surface recording electrodes, and a twisted pair of fine stainless steel wires was introduced stereotaxically into the right dorsal hippocampus (2.1mm posterior from bregma; 1.5mm from the midline; 1.8mm deep from the cortical surface). Electrodes were attached to a micro-plug, and cemented to the cranium with dental acrylic. Behavior and EEG were simultaneously recorded from freely-moving animals; mice were monitored for 4-5 hours/session, for 3-6 sessions over the course of 2 weeks.

Immunoblot analyses of brain proteins

Intact brains from wild-type and Kv1.1$^{-/-}$ littermates were homogenized and a crude membrane fraction was prepared as previously described by Trimmer (1991). In brief, brains were homogenized in 5 mM phosphate buffer (pH 7.4) containing 320 mM sucrose and 100 mM NaF. The homogenate was centrifuged at 800*g* for 10 minutes to remove nuclei and unbroken tissue, and the resultant supernatant centrifuged at 100,000× *g* for one hour to prepare a crude membrane fraction. Equal amounts of membrane protein (10 μg per lane) were electrophoretically size-fractionated on 9% SDS polyacrylamide gels and transferred to nitrocellulose membranes. The resulting blots were incubated with different mouse monoclonal antibodies (NeuroMab, Davis, CA (www.neuromab.org) used at 2 μg/ml), washed and then incubated with HRP-conjugated secondary antibodies (ICN, Cleveland, OH) followed by enhanced chemiluminescence reagent (Perkin Elmer, Wellesley, MA). Immunoreactive bands were visualized by exposing the blots to X-ray film.

Viral Vector Delivery

A non-pathogenic herpes simplex virus (HSV1) amplicon vector was used. The vector contained either the *E.coli lacZ* gene alone (to express beta-galactosidase (β-gal) as a reporter molecule) or both *lacZ* and the gene for the rat *Kcna1* subunit. Details of the viral vector preparation have been published (Lee et al., 2003). Previous studies demonstrated more than 98% co-expression of transgene and reporter gene in this system, with the vector showing a >4-fold preference for infecting neurons over glia (Fink et al., 1997; Lee et al., 2003). Animals were anesthetized with 2% isoflurane and positioned in a stereotaxic frame. Viral vectors were injected bilaterally (15×10^3 vector particles and 25×10^3 helper virus particles/injection) at two sites per hemisphere (injection volume of 1.2μl per site), into the dentate gyrus/CA3 region of the dorsal and/or middle hippocampus. For dorsal hippocampus, coordinates for injection were: posterior from bregma 2.1, lateral from midline 1.5, depth from cortical surface 1.8; for the middle hippocampus, coordinates were AP-2.8, L +/−3.3, V −4.0. The vectors were delivered at a rate of 0.2μl per minute over 5 minutes, using a 10μl Hamilton syringe. A total of 31 mice were injected.

Tissue Preparation for Light Microscopy/Immunocytochemistry

General tissue preparation—Animals were anesthetized with sodium pentobarbital (100 mg/kg, i.p.) at the predetermined age or survival time, then perfused with isotonic saline with heparin (1000 units/ml saline), followed by a solution of 4% paraformaldehyde (PFA) in 0.1M sodium phosphate buffer (PB; pH 7.4), 0.05 % glutaraldehyde and 1% picric acid and/or 4% PFA only. The brains were immediately removed and placed in the same fixative for 1-4 hours at 4°C. After post-fixation, the brains were rinsed in PB, cryoprotected in 10% sucrose in 0.1M PB for 1 hour, followed by 30% sucrose in 0.1M PB for 24 hours at 4 °C, then frozen on dry ice. Thirty μm transverse serial sections were cut on a sliding microtome equipped with a freezing stage, then selected for further processing which included: cresyl violet staining for general histological evaluation; immunocytochemistry for neuronal and glial cell markers and for Kv1.1 protein; histochemistry for zinc (Timm staining) and for β-galactosidase (X-gal staining); and Fink-Heimer staining for degenerated neurons and axonal terminals. Sets of coronal sections representing different antero-posterior levels of the hippocampus were sampled (for details see Wenzel et al., 2001).

Immunocytochemistry—Immunocytochemical methods were used to characterize the seizure-induced pathologies in Kv1.1 −/− mice, to localize the distribution of Kv1.1 channels in hippocampal neurons of wild-type mice, and to determine localization of newly expressed Kv1.1 channels following HSV infection in Kv1.1 −/− mice. Subsets of alternate sections were processed for immunocytochemistry (ICC) using a modification of the avidin-biotin complex

(ABC)-peroxidase technique (Hsu et al., 1981), and performed as previously described (Wenzel et al., 2004). Briefly, sections were rinsed in PB, followed by 0.1M Tris-HCL buffer (TB) (pH 7.4); endogenous peroxidases were then inactivated by treatment with 0.5-1% H_2O_2 in TB for 2 hours. Sections used for Kv1.1 ICC were pretreated with 0.1-1.0% sodium borohydride and/or microwaved in 10mM citric acid buffer. Sections were then treated with 3-5% bovine serum albumin (BSA) (Boehringer Mannheim, Indianapolis, IN), 3% goat or horse serum (Sigma, St.Louis, MO) and 0.3% Triton X (TX) (0.25% DMSO for Kv.1.1 ICC) in 0.05M TB, 0.15M NaCl, pH 7.4 (TBS) for 1 hour to reduce nonspecific staining. Sections were rinsed in TBS for 30 minutes and incubated for 24 hours at 4° C in the various antibodies and dilutions [mouse anti-β-galactosidase, (Chemicon, Temecula, CA), 1:1000; rabbit anti-cow *G*lial *F*ibrillary *A*cidic *P*rotein (GFAP), (DAKO Corporation, Carpinteria, CA), 1:4000; and poly- and monoclonal antibodies against Kv1.1 and Kv1.4 (Rhodes et al., 1995; 1997), 1:750 and 1:50, respectively] in TBS containing 1% goat or horse serum, 2% BSA and 0.3% TX (0.3% DMSO for electron microscopy). Anti-Kv1.1 (K20/78), anti-Kv1.2 (K14/16) and anti-Kv1.4 (K13/31) mouse monoclonal antibodies used in this study are available from NeuroMab (www.neuromab.org), a not-for profit supplier of monoclonal antibodies administered through the University of California. Following rinses for 2 hours in TBS, sections were incubated in biotinylated goat anti-rabbit IgG or horse anti-mouse IgG (Vector Laboratories, Burlingame, CA), diluted 1:500 for 24 hours at 4° C, rinsed 2 hours in TBS and then incubated in ABC (Elite ABC Kit, Vector Laboratories, Burlingame, CA), diluted 1:500 in 1% goat or horse serum, 2% BSA, 0.3% TX/DMSO and TBS for 24 hours at 4° C. Sections were rinsed thoroughly in TB (pH 7.6), and then incubated for 15 minutes in 0.025% 3,3'-diaminobenzidine (DAB, Sigma, St. Louis, MO) in TB. After reacting for 5-10 minutes in fresh DAB with 0.003% H_2O_2, sections were rinsed in TB, followed by PB. Specificity of the immunostaining was evaluated by omitting primary antibodies from the regular staining. Sections were mounted on slides, dehydrated, cleared, and coverslipped with Permount.

For double-label immunofluorescence staining, sagittal brain sections (40 μm thick) were cut on a freezing stage sliding microtome. Free-floating sections were treated with 10% goat serum in phosphate buffer containing 0.3% TX-100 (vehicle), and then incubated them overnight at 4°C in vehicle containing different combinations of mouse monoclonal antibodies of different IgG isotypes. Sections were incubated in isotype-specific Alexa-conjugated secondary antibodies (Invitrogen, Carlsbad, CA) as described previously (Strassle et al., 2005).

Timm staining—The Timm method for staining heavy metals was used for the detection of synaptic vesicular zinc (particularly enriched in hippocampal mossy fiber boutons). After initial perfusion fixation with 4% PFA, the brains were transferred to a solution containing 3-4% glutaraldehyde, 0.1% Na_2S, and 0.136 mM $CaCl_2$ in 0.12 M Millonig's PB, pH 7.3, for 48 hours at 4° C, followed by cryoprotection in 30% sucrose. Frozen sections were cut at 30 μm and then mounted on slides, air-dried and then transferred to a fresh developer solution containing 30 ml gum Arabic (50%), 5 ml 2 M citrate buffer, 15 ml hydroquinone (5.76%) and 250 μl silver nitrate (0.73%) for 1 hour in the dark. Sections were counterstained with cresyl-violet, dehydrated, cleared in toluene and coverslipped.

X-Gal staining—Following vector delivery of the *E.coli lacZ* gene, reporter expression becomes evident 2-4 hours post-transfection, increases to a maximal plateau at 12-72 hours, and declines to undetectable levels by about 5 days (Lee et al., 2003). At predetermined survival times, the brains of the experimental animals were perfused with 4% PFA and postfixed for 4 hours in the same solution, then cryoprotected and sectioned at 30μm. Sections were then rinsed in 0.1M PB, permeabilized with a solution containing 0.02% sodium deoxycholate and 0.1% NP40 (Sigma/Aldrich, St. Louis, MO, and Fluka Biochemica, Switzerland, respectively). Following rinse in 0.1M PB, sections were stained with X-Gal (5-Bromo-4-Chloro-3-Indolyl-β-D-Galactopyranoside; Sigma/Aldrich) by incubation in a solution, which consisted of K-

ferricyanide(I) 5mM, K-ferrocyanide(II) 5mM, $MgCl_2$ 2mM, and X-Gal 1mM in 0.1 saline PB, for 8-12 hours. X-Gal-positive staining was indicated by presence of blue-stained neurons.

Fink-Heimer degeneration staining—Sections were stored at least 1 week in 5-10% formalin, then rinsed in 0.1 M PB, treated with 0.5% potassium permanganate, and bleached with 1% oxalic acid and 1% hydroquinone. The sections were then impregnated with 0.6% $AgNO_3$ in 0.1% uranyl nitrate, then with 1.5% $AgNO_3$ in 0.2% uranyl nitrate, followed by ammoniacal silver nitrate solution (containing 2.5% $AgNO_3$ in 0.1% NaOH and 1.2% NH_4OH), then reduced twice in 0.03% citric acid and 0.3% formalin in 9.5% ethanol. Finally, the sections were treated with 0.5% sodium thiosulfate, rinsed, mounted on gelatine-coated slides, and coverslipped.

Pre-embedding immunocytochemistry and electron microscopy

For electron microscopic analysis, pre-embedding ICC for anti-Kv1.1 channel protein was used. Hippocampal sections containing Kv1.1-positive neurons and/or axons (in CA3 stratum lucidum or dentate molecular layer and hilus), as seen at the light level, were selected. Sections were rinsed in PB and post-fixed in 1% osmium tetroxide in 0.15M PB, pH 7.4, for 1 hour at room temperature, followed by alcohol dehydration, and flat embedding in Eponate 12 resin (Ted Pella, Redding, CA) between two aclar sheets. After polymerization at 60°C, selected areas of the sections containing immuno-stained cells or processes were remounted on plastic blocks, then trimmed; serial thin sections were cut, stained with uranyl acetate and lead citrate, and examined with a Philips CM120 electron microscope.

Quantitative Analyses

Assessment of neuronal cell loss/Stereological cell counts—Unbiased stereological techniques - as described previously (Zhao et al., 2003) - were used to estimate the number of neurons in the right dentate hilus of wildtype mice (n=4), and two groups of Kv1.1 knock-out mice; one $Kv1.1^{-/-}$ group (n=4) experienced mild/moderate seizures but no prolonged, severe seizure episodes were observed. The other $Kv1.1^{-/-}$ group (n=4) were observed to have experienced episodes of status epilepticus (n= 4). In sections from all animals, hilar cell number and volume were measured. The hilus was defined by its borders with the granule cell layer and by two straight lines connecting the proximal end of the CA3 pyramidal cell layer with the tips of the dorsal and ventral blades of the granule cell layer. Only healthy-appearing neurons were counted; degenerating neurons (i.e.., cells exhibiting apoptotic bodies and/or microvacuolation) - frequently observed in status epilepticus animals - were excluded. The stereological procedure involved a systematic collection of seven evenly spaced sections through the entire region of interest (ROI). From brains cut into 30 μm coronal sections, every section was collected to encompass the entire ROI (i.e., the dentate hilus of the dorsal hippocampus between bregma −1.46mm and −2.36mm (Franklin & Paxinos, 1997)). Every fifth section was stained and the ROI area in each section was measured. Regional area was estimated with suitable precision by applying a point grid with a known area associated with each point. Region volume was then calculated using the Cavalieri method (Gundersen & Jensen, 1987). The grid generation and volume calculations were performed with Stereologer™ (Version 1.3) software, using a Nikon E600 microscope with motorized xyz stage controller (ASI MS-2000). Unbiased cell counting was performed using the optical fractionator stereological method (West et al., 1991) (which calculates the total number of objects in the entire reference space by summing the objects sampled in the individual dissectors and multiplying by the reciprocals of the sampling fractions for section, area, and thickness of the reference space).

Mossy fiber synaptic reorganization—Mossy fiber reorganization was evaluated by scoring the distribution of Timm-stained granules in the dentate granule cell layer and

supragranular region (i.e., the most inner part of the inner third of the dentate molecular layer), as previously described (McKhann et al., 2003). Following Tauck and Nadler (1985), we scored sections with no or only occasional Timm granules in the GCL and/or in the supragranular region as 0. Sections with scattered Timm granules throughout the GCL and within the supragranular region were given a score of 1. Sections that exhibited either patches of heavily-stained mossy fibers interspersed with regions of sparser staining or a continuous band of low staining intensity within the supragranular region, were given a score of 2. Sections with a dense, continuous band of supragranular mossy fiber staining that extended into, or covered the entire IML, were scored as 3.

Statistical analysis—Cell counts from stereological estimates were analyzed using separate one-way ANOVA between experimental animal groups. The Bonferroni multiple comparison test was used to make individual comparisons while holding experiment-wise error rate to 0.05. Precision of cell number estimates and precision of ROI volume estimates were calculated using coefficient of error (CE), with Stereologer™ software (MicroBrightfield, Inc., Williston,VT).

Results

General Morphology

Brains of Kv1.1 knock-out mice appeared histologically normal, and did not present with gross developmental defects when compared with wild-type mice. However, the average brain weight of adult (2-5 month old) Kv1.1$^{-/-}$ mice was approximately 20% greater than the brain weight of wild-type mice (Smart et al., 1998; Persson et al., 2007). Immunocytochemistry for the Kv1.1 α subunit confirmed the complete absence of Kcna1 immunoreactivity (reflecting absence of channel expression) in the knock-out mouse, and the characteristic pattern of subunit expression in the wild-type animal (cf. A and B in Fig. 1).

Observation of seizure behaviors and EEG monitoring

The seizure phenotype resulting from *Kcna1* gene deletion has been previously described (Smart et al., 1998; Rho et al., 1999). In brief, during the second-to-third postnatal week, Kv1.1$^{-/-}$ mice begin to exhibit seizure-like behaviors (e.g., episodic eye blinking, twitching of vibrissae, forelimb paddling, arrested motions and hyper-startle responses (Smart et al., 1998)). These behaviors progress into spontaneous generalized seizures by 4-5 weeks postnatal. Generalized tonic-clonic seizures typically begin with tonic arching and tail extension, followed by forelimb clonus (or rearing and forelimb clonus), and then generalized synchronous forelimb and hindlimb clonus; seizures are typically followed by a period of post-ictal depression (Rho et al., 1999).

As reported earlier (Smart et al., 1998), a large percentage (>50%) of the Kv1.1$^{-/-}$ mice do not survive beyond 5-6 weeks postnatal (the exact percentage is sensitive to background strain); death is thought to be due to cardiac and/or respiratory failure associated with severe generalized seizure activity lasting for several hours (i.e., status epilepticus). Mice that survive beyond 5-6 weeks of age continue to exhibit spontaneous seizures. In our study, seizure activity in these long-term survivors (some surviving for more than 12 months) was generally of lesser intensity than seen in animals that died at earlier ages. Seizure-associated electrical brain activity in Kv1.1$^{-/-}$ mice was monitored from skull (cortical surface) and depth (hippocampal) electrodes in 8 mice (4 wild-type and 4 Kv1.1$^{-/-}$) from which subsequent histology was obtained. Seizure monitoring was also carried out in an additional 17 animals (8 wild-type and 9 Kv1.1$^{-/-}$) from which no subsequent histology is available. Seizure-like EEG patterns appeared at both recording sites; often onset appeared “simultaneously” so that it was not possible to determine a focal onset. However, in a few cases, the onset of a seizure EEG pattern

in the depth recording preceded ictal-like activity on the surface. Figure 1E shows an example of such a seizure, with EEG recording from a Kv1.1$^{-/-}$ mouse during "interictal" activity (top traces from surface and depth) and leading into a spontaneous tonic-clonic seizure event (accompanied by facial clonus, rearing and falling, forelimb and hindlimb clonus, and generalized tonic-clonic activity). Pre-seizure interictal "spikes" were seen particularly in the surface (Cortex) lead (asterisks). The ictal episode began with abrupt voltage depression in the depth (Hippocampus) lead (black arrowhead), with activity progressing into high-amplitude fast spiking activity which increased in amplitude and was then maintained for several seconds (both surface and depth). High amplitude EEG seizure discharge stopped abruptly (blue arrowhead), with EEG flattening; occasional brief discharges were then superimposed on the EEG (particularly in hippocampus) until a normal EEG pattern was restored. Ictal episodes typically lasted 40-100 seconds, and behavioral changes were usually associated with abnormal ictal electrical activity. However, in some animals, ictal EEG patterns were observed in the absence of obvious behavioral changes. None of the wild-type mice displayed either EEG or behavioral seizure patterns.

Seizure-related neuropathology

While seizure phenotype had been previously described for the Kv1.1 knock-out mouse, that description has to date lacked a correlative neuropathological characterization. We therefore examined histopathological features in hippocampus of Kv1.1$^{-/-}$ mice, with attention to patterns of neuronal damage, gliosis, and mossy fiber sprouting. Initial qualitative assessment of Nissl-stained and ICC-prepared material was based on observations of 24 mice. These observations suggested obvious neuronal loss in hippocampal subfields, dentate hilus, thalamus and other cortical regions of adult Kv1.1$^{-/-}$ mice compared to age-matched normal controls. The changes were quite variable from animal to animal. When neuropathology was examined in relation to behavioral seizure observations, it became clear that significant (i.e., qualitatively obvious) neuropathology was seen primarily in animals with documented status epilepticus (SE). This relationship was relatively independent of age. For example, 10 week old Kv1.1$^{-/-}$ mice that were observed to have experienced status epilepticus (i.e., prolonged severe seizures lasting more than 10 minutes) consistently exhibited widespread damage in large portions of the hippocampal subfields CA1 and CA3 (Fig. 2B, E). Although our observation period was limited (and it was therefore impossible to quantify total time in seizure), it is likely that these particular animals experienced additional severe seizures. In the mice with status epilepticus, neuronal loss seen in Nissl-stained sections corresponded to extensive and intense degenerative profiles (cell bodies and axonal terminals) within the same hippocampal subregion, as revealed by Fink-Heimer staining (Fig. 2C, D). In the hilus of Kv1.1$^{-/-}$ mice, degeneration of hilar interneurons and mossy cells was reflected in axonal terminal degeneration in the cells' fields of termination (e.g., mossy cell terminal degeneration in the dentate inner molecular layer; terminal degeneration associated with dentate interneuron subpopulations in the outer molecular layer) (Fig. 4D). Animals which had experienced status epilepticus and were sacrificed at 1-2 month of age also exhibited neuronal cell death and extensive terminal degeneration (as detected in cresyl violet and Fink-Heimer staining), often involving brain regions in addition to hippocampus (e.g., neocortex, piriform cortex, thalamus, amygdala) (Fig. 3A-D). In contrast to such severe neuropathological changes, animals sacrificed at 2-5 months that showed (during our limited observation periods) few and/or mild seizures - e.g., only "early stage" seizures (immobilization, vibrissae twitching or forelimb clonus) or a generalized seizure lasting for only a few seconds - typcially exhibited little cell loss and/or degenerative changes.

These qualitative observations were confirmed in a subset of control and Kv1.1 knock-out mice (n=4/group) subjected to quantitative stereological analysis of the hilus (a region particularly sensitive to cell loss). In these animals, total hilar cell number in SE Kv1.1$^{-/-}$ mice was much

lower than in controls or in non-SE Kv1.1$^{-/-}$ mice (Table 1). Cell number in non-SE Kv1.1$^{-/-}$ mice was slightly less than in controls (statistically insignificant), suggesting that even a low level of ongoing seizure activity could affect cell viability. Interestingly, hilar volume was much larger in Kv1.1$^{-/-}$ mice (both SE and non-SE Kv1.1$^{-/-}$ mice), consistent with the generally higher brain volume and weight in the knock-outs. Given this disparity, neuronal cell density was much lower in Kv1.1$^{-/-}$ mice.

The expression of GFAP immunoreactivity in hippocampal astrocytes was used as a marker for reactive astrocytosis. Astrocytes were defined as "reactive" when their GFAP-stained cell bodies were hypertrophic and they had large processes (more than two times thicker in diameter than normal and/or with expanded processes (McKhann et al. 2003)). In the Kv1.1$^{-/-}$ mice, the degree of reactive astrogliosis varied considerably across animals, again depending upon seizure severity, duration, and frequency. All of the Kv1.1$^{-/-}$ mice sacrificed at 2-5 months of age, that had experienced seizures episodes since early in postnatal life showed striking up-regulation of GFAP expression (Fig. 2F-H). In animals observed to have infrequent and mild seizures (e.g., one seizure per 2-3 hours of observation time), the patterns of GFAP expression typically reflected mild gliosis in distinct hippocampal regions (particularly the dentate gyrus/hilus and CA3 subfields). In all animals observed to have experienced status epilepticus, there was extensive astrogliosis throughout the hippocampus as well as in other brain regions (e.g., neocortex, piriform cortex, thalamus, amygdala).

This relationship between SE and neuropathology held also for older mice, >10 months at time of sacrifice. Even in these old animals, mild seizure activity over many months (as determined by our limited observational samples) was correlated with only minor cell loss (apparent as thinning of the CA1 pyramidal cell layer, and mild terminal degeneration within the CA1 subfield and the dentate hilus) and restricted regions of reactive astrocytes (dentate gyrus/hilus and CA3 subfield) (Fig. 4A, C, E). In comparison, younger (10 week old) Kv1.1$^{-/-}$ mice that had experienced severe, prolonged generalized seizures (SE) exhibited the severe neuropathologies described above (Fig. 4B, D, F).

We also evaluated (with Timm staining) mossy fiber sprouting in Kv1.1$^{-/-}$ and wild-type mice. In the latter, mossy fiber staining was generally restricted to the dentate hilus and the hippocampal CA3 subfield (suprapyramidal stratum lucidum and proximal infrapyramidal s.oriens in CA3c) (Fig. 4G, I); in some cases, very sparse Timm staining could be seen in the granule cell and inner molecular layers at the dentate crest. In Kv1.1$^{-/-}$ mice, mossy fiber staining was variable in location and intensity. Mossy fiber sprouting into the inner molecular was observed as early as 5 weeks postnatal. Some animals, at 5 months of age, exhibited extensive mossy fiber sprouting across the entire dentate inner molecular layer (Fig. 2H, J). In addition to the appearance of mossy fibers in the inner molecular layer, other evidence of "sprouting" included Timm staining within the granule cell and CA3 pyramidal cell layers, and the extension of infrapyramidal (s.oriens) Timm staining into CA3b. Robust mossy fiber sprouting correlated with other neuropathological features such as marked neuronal cell loss and gliosis, as well as with severe seizure activity (SE). Kv1.1$^{-/-}$ mice observed to have only mild seizure activity (even those at 10-12 months) showed only moderate mossy fiber sprouting – i.e., sparse Timm staining localized to the granule cell and inner molecular layers. A semi-quantitative analysis of mossy fiber sprouting is presented in Table 1.

Localization of Kv1.1-containing channels in the hippocampus

Previous immunocytochemical and electron microscopic (EM) studies of Kcna1 expression and localization in the mouse brain/hippocampus focused on the dentate molecular layer and CA3/hilar region, where this channel subunit appears to be expressed at high density. Channels containing the Kv1.1 α subunit were shown to localize to juxtaparanodal regions of myelinated axons, and unmyelinated axons and synaptic terminals, and thought to be associated with CA3

pyramidal neurons and interneurons (Wang et al., 1994). Subsequent light microscopic studies on the rat hippocampus, using immunocytochemistry and lesion techniques, revealed an association of Kv1.1 α subunit expression/localization with axonal fiber tracts within, and afferent to, the hippocampus (Monaghan et al., 2001). Immunocytochemical patterns of Kcna1 staining closely matched the termination zones of entorhinal afferents into the hippocampus as well as the mossy fiber pathway (Rhodes et al. 1997; reviewed by Trimmer and Rhodes, 2004). A detailed ultrastructural analysis of Kv1.1 α subunit localization to the various compartments of axonal pathways in the hippocampus has not yet been reported.

In the present study, we have therefore expanded previous descriptions of Kv1.1 α localization. Light and electron-microscopic observations were made on tissue from 15 wildtype mice. The ultrastructural analysis of Kv1.1 α channel protein expression in hippocampal neurons and pathways provides a background for assessing Kv1.1 α subunit expression following gene transfer into the hippocampus of $Kv1.1^{-/-}$ mice (see below). A low magnification photomicrograph of the hippocampal formation in a wild-type mouse shows the characteristic pattern of immunohistochemical Kcna1 expression (Fig. 1A). Of particular note are the following features of this pattern: a) There is a band of intense Kcna1 immunoreactivity in the middle molecular layer of the dentate gyrus, distinct from less intense immunoreactivity of the outer and inner molecular layers; this zone of prominent Kcna1 immunoreactivity corresponds to the termination field of the medial perforant path. b) There is no Kcna1 immunoreactivity in granule cell bodies (Fig. 5A). c) Positive Kcna1 immunostaining is observed in some neuronal cell bodies in hilus and dentate layers; these cells appear to constitute a subpopulation of interneurons (Fig. 1A). d) The prominent hilar immunoreactivity pattern continues as two fiber bundles, above and below the CA3 pyramidal cell layer, which correspond to the supra- and infrapyramidal mossy fiber tracts (in s.lucidum and proximal s.oriens, respectively). e) Kcna1 immunoreactivity is also present in the distal strata oriens and radiatum of the CA3/CA1 subfields, but the density is lower than in s.lucidum and proximal s.oriens (Fig. 1A). f) The s.lacunosum and adjacent distal portions of s.radiatum in the CA1 subfield, usually associated with the termination zone of Schaffer collaterals, show high levels of Kv1.1 α channel expression. However, little Kcna1 immunoreactivity is observed in the outer dentate molecular and CA1/CA3 distal molecular layers, regions associated with the termination field of axons from lateral entorhinal cortex neurons in lamina II and III. g) As in the dentate, subpopulations of CA1 presumed interneurons show intense somatic Kcna1 immunoreactivity (Fig.1C).

At the electron microscopic level, Kv1.1 α channel protein expression can be seen, as electron-dense immunoreaction product, in various axonal components of the major hippocampal pathways. The prominent light-microscopic Kcna1 staining in the dentate middle molecular layer corresponds to an intense staining pattern at the electron microscopic level; immunoreactivity is localized predominantly to axonal membranes, with lesser immunoreactivity in the axoplasm (Fig. 5C). In myelinated hippocampal axons (e.g., fimbria hippocampi, alveus), Kcna1 immunoreactivity is present within the juxtaparanodel region (Fig. 5B), as previously described in axons from brain stem (Wang et al., 1993,1994); no Kcna1-specific immunostaining is observed within the node of Ranvier. Kcna1 immunoreactivity is also seen in axonal terminals, often in synaptic contact with dendritic spines (Fig. 5D, E). We found no evidence for Kcna1 immunoreactivity in granule cell dendrites.

The prominent Kcna1 staining seen in the dentate hilus and CA3 s.lucidum at the light microscopic level is reflected in ultrastructural evidence of high levels of Kcna1 expression in mossy fiber axons, in both hilus and CA3 (Fig. 5F). Despite this strong immunoreactivity in the granule cell axons, we found no Kcna1 immunoreactivity in mossy fiber boutons (Fig. 5F). Kcna1 immunoreactivity is also found in small axons within the hilus and CA3 s.oriens, suggesting that recurrent axons of CA3 pyramidal neurons, and axons from local interneurons

with positive cell body staining, express Kv1.1-containing channels (Fig. 5E). In CA1, electron microscopic data reveals Kv1.1 α subunits localized to axons and axonal terminals, with strong immunoreactivity in s.lacunosum. As also seen for granule cells, there is no Kcna1 immunostaining in CA1 pyramidal cell somata and/or dendrites (data not shown).

Lack of compensatory changes in ion channel expression in Kv1.1−/− mice

Genetic elimination of subunits of functional protein complexes critical to regulating neuronal activity, as is the Kv1.1 α subunit, can often result in compensatory changes in expression of proteins of similar/overlapping function (Inchauspe et al., 2004) or in the stoichiometry of subunit components within the protein complex (Christensen et al., 2004; Ogris et al., 2006; Menegola & Trimmer, 2006). We determined the effects of the targeted deletion of *Kcna1* on the expression levels of different Kv α and auxiliary subunits, and Kv-channel associated proteins. This analysis included subunits co-assembled in Kv1.1-containing complexes (Kv1.2, Kv1.4, Kvβ2), and those in (or associated with) distinct channel complexes that also act to regulate neuronal excitability (Kv1.3, Kv2.1, Kv3.1, Kv4.2, PSD-95) (data not shown). Immunoblot analyses of wild-type and Kv1.1$^{-/-}$ mouse brain membrane proteins revealed no differences in overall expression level (Fig. 6A). The lack of compensatory changes in other Kv channels (based on observations in 10 Kv1.1$^{-/-}$ mice) – and particularly in Kv1.4, which is a critical component of the axon channel in which Kv1.1 participates (Fig. 6B) - may contribute to the strong seizure phenotype of the Kv1.1$^{-/-}$ mice. Double immunofluorescence staining of wild-type and Kv1.1$^{-/-}$ hippocampus with subtype-specific monoclonal antibodies against Kv1.1, Kv1.2 and Kv1.4 revealed a similar lack of compensatory changes. While a complete loss of Kv1.1 immunoreactivity was observed in the Kv1.1$^{-/-}$ hippocampus, immunofluorescence staining for Kv1.2 and Kv1.4 was not substantially altered relative to wild-type (Fig. 6C). However, a dramatic expansion of the boundaries of Kv1.4 staining was observed in the Kv1.1−/− hippocampus, consistent with expansion of CA3 stratum lucidum and dentate hilus expansion as seen in immunoperoxidase and Timm staining (see also hilar volume measurements presented above). It should be noted, however, that although no compensatory subunit changes were seen in analysis of whole brain or whole hippocampus tissue, a similar analysis has not yet been carried our for individual neurons or sub-sets of specific neuronal subtypes in focal brain regions. The relative abundance and/or distribution of related channel subunits may indeed have changed – and led to channel formation consisting of aberrant combinations of subunits – in some neurons. This possibility – and its potential functional implications – remain to be explored.

Light- and electron microscopic investigations of Kv1.4 distribution patterns in wild-type mice revealed colocalization of Kv1.1α and Kv1.4 α subunits to the same axonal compartments of hippocampal neurons - i.e., in axons of the major hippocampal pathway neurons in the dentate gyrus and hippocampus (Fig. 5H, I) – and this Kv1.4 distribution remained similar in the Kv1.1$^{-/-}$ mouse (Fig. 6B). Therefore, at least for Kv1.4, the likelihood of there being a cell type-specific subunit compensatory change seems unlikely.

Viral vector-mediated gene expression

Expression of genes introduced by viral vector infection in the brains of Kv1.1$^{-/-}$ mice was assessed by histochemistry to visualize β-galactosidase (β-gal) (the gene product of *lacZ*) and immunocytochemistry for the Kcna1 subunit protein. Animals injected with vectors carrying only *lacZ*, or *lacZ* plus *Kcna1*, were sacrificed 3-9 days after vector delivery. Injections of vector targeted the CA3 region and the dentate hilus in the dorsal and middle hippocampus (representative injection site shown in Fig. 7A). Vector delivery resulted in successful cell infection (i.e., numerous labeled cells seen in several histological sections) in ~30% of the Kv1.1$^{-/-}$ mice (Table 2). Infected neurons were detected within and around the injection site (a diameter of several hundred microns), and in most cases restricted to hippocampus. The

expression of the marker gene product, β-gal, was visualized histochemically by the blue reaction product of X-Gal processing (Fig. 7), and confirmed with β-gal immunocytochemistry. Vector infection appeared to be preferentially for granule cells (Fig. 7B, C, E), although some CA3 pyramidal neurons (Fig. 7D, F) were also infected. The vector did not infect glia. High expression of the marker molecule completely stained cell bodies, dendrites and axonal projections (Fig. 7B-F). Granule cell axonal staining was reflected in a punctate (terminal) pattern in hilus and strata lucidum and oriens of the CA3 subfield (Fig. 7B, D).

Expression of the exogenous Kv1.1 gene product in the hippocampus from Kv1.1 knockout mice (mice injected with the viral vector carrying both *lacZ* and *Kcna1*) was analyzed in tissue sections processed immunocytochemically for Kcna1 protein. In these sections, Kcna1 immunoreactivity was detected in a relatively small number of neurons (granule cells (Fig. 8A, B) and some CA3 pyramidal neurons (Fig. 8C, D)) compared to the widespread pattern of X-Gal-stained neurons. However, when compared to the number of with β-gal IR cells, the Kcna1 numbers were similar (data not shown). In Kcna1-immunopositive cells, immunoreactivity was seen in somata, dendrites and axons – a pattern rather different from the exclusive axonal localization of Kv1.1 in wild-type granule cells and pyramidal cells. In infected neurons, Kcna1 immunoreactivity often extended into dendritic spines and axonal varicosities (Fig. 8B, D). These light microscopic observations were supported by Kcna1 localization at the electron microscopic level. Low magnification EM revealed prominenet Kcna1 expression in single granule cells (Fig.9A); high levels of intracellular subunit immunopositivity was present in somata (Fig. 9B), dendrites (Fig. 9b, C, D) and mossy fiber axons (Fig. 9G). Within a given neuron, the intensity of Kv1.1 immunoreactivity was highest on the somatic and dendritic cell membrane (Fig. 9D, E), and somewhat lower in the cytoplasm of processes and dendritic spines (Fig. 9F).

Discussion

Localization of Kv1.1α-containing channels and their role in neuronal excitability

Voltage-gated potassium channels play a critical role in neurotransmission in central and peripheral neurons; because of their diverse localizations, complex subunit compositions, and subunit-distinct gating properties, they influence a variety of neuronal (and glial) processes, from baseline excitability to action potential firing patterns to modulation of synaptic transmission (Shieh et al., 2000; Geiger and Jonas, 2000; Hille, 2001; Dodson and Forsythe, 2004; Trimmer and Rhodes, 2004). The *Shaker*-type potassium channels were among the first identified (initially in *Drosophila* – Tempel et al., 1987) and have been intensively studied. The Kv1 α subunits (Kv1.1, Kv1.2, Kv1.4) are abundantly expressed in the brain, and are found predominantly in heteromeric channel complexes (Wang, et al., 1994; Trimmer and Rhodes, 2004). Importantly for understanding the Kv1.1 knockout mouse, native channels composed of homomeric Kv1.1 subunits appear to be quite rare. In the hippocampus, Kv1.1, Kv1.2, and Kv1.4 are co-expressed in the dentate middle molecular layer, associated with the axonal termination of the entorhinal medial perforant path (Sheng et al., 1993; Wang et al., 1994; Rhodes et al., 1997; Monaghan et al., 2001). Colocalization of these three subunits has been also demonstrated in CA3 axons (e.g., Schaffer collaterals) (Monaghan et al., 2001). However, in mossy fiber axons, only Kv1.1 and Kv1.4 colocalize (Sheng et al., 1992; Cooper et al., 1998; reviewed in Rhodes and Trimmer, 2004). Further, both our present findings and results of previous electron microscopic immunocytochemical studies (Wang et al., 1994; Cooper et al., 1998) have shown that Kv1.1, Kv1.2 and Kv1.4 subunits are concentrated at the axonal membrane near presynaptic terminals of all major intrinsic excitatory hippocampal connections, suggesting a critical role for these Kv1-containing channels in synaptic depolarization and neurotransmitter release (Trimmer and Rhodes, 2004).

Given this localization, it appears that channel deletion would certainly given rise to abnormal electrical activity. What is not so clear, however, is whether the loss of only one subunit type – say Kv1.1 – would necessarily lead to loss of channels (or channel function) from the characteristic axonal and terminal zones. Our current study does show that even in the Kv1.1 knockout mouse, Kv1.4 can be seen in appropriate locations in hippocampus. Moreover, on the basis of whole brain/whole hippocampus analysis, we have found that there is no obvious compensation of other component subunits of Kv1.1-containing channels, or of other Kv channel subunits that may compensate for the loss of Kv1.1. Loss of Kv1.1 subunits from these axonal/terminal locations gives rise to epileptic behavior (Smart et al., 1998), to a decreased seizure threshold even in the heterozygous animal (i.e., with a 50% reduction of Kv1.1 subunits (Smart et al., 1998), and to aberrant electrical discharge patterns in hippocampal neurons (Lopantsev et al., 2003).

The *megencephaly* mouse (*mceph/mceph* - Donahue et al., 1996) is also based on a *Kv1.1* mutation (a spontaneous 11 base pair deletion) that expresses a truncated Kv1.1 protein (MCEPH protein) (Petersson et al., 2003). This abnormal protein is expressed in cells throughout the brain, where it is trapped within the endoplasmatic reticulum (Persson et al., 2005). In addition to general brain hypertrophy, the *mceph/mceph* mouse shows complex partial seizures (as in the Kv1.1 knock-out mouse), and disturbances in expression of several trophic molecules. Persson et al. (2007) and Almgren et al. (2007) have also recently reported that the hippocampus (and ventral cortex) of Kv1.1$^{-/-}$ mice is significantly enlarged, and our data are in agreement with that finding. These authors have now shown that the hypertrophy in *mceph/mceph* and Kv1.1$^{-/-}$ mice is due to an increase in neuronal (and glial) cell numbers (Almgren et al., 2007). However, our cell count analysis in the dentate hilus showed a significant *loss* of cell number in Kv1.1$^{-/-}$ mice (relative to wild-type mice) that had experienced status epilepticus, and a small (insignificant cell loss in the non-SE Kv1.1$^{-/-}$ group), a difference we attributed to seizure-related damage. Intriguingly, Kv channel dysfunction has been shown to result in increased cell proliferation and reduced apoptosis (O'Grady & Lee, 2005), a mechanism that might help explain abnormal brain growth in *mecph/mceph* and Kv1.1$^{-/-}$ mice. Further, seizure activity is known to result in neurogenesis in adult rodents - but cell loss in immature animals (Liu et al., 2003). Given our data on apparent cell loss associated with seizures, and given the fact that the *mecph/mceph* mouse also is said to exhibit spontaneous seizure activity, a careful examination of neuronal - and glial – cell numbers is required, particularly with respect to different developmental timepoints and seizure frequency/severity.

The Kv1.1 knock-out mouse as a model of TLE

Kv1.1 knock-out mice exhibit frequent spontaneous seizures - both behavioral and electrographic (Smart et al., 1998; Rho et al., 1999). Although the *Kcna1* gene is widely distributed throughout the mouse brain, *Kcna1* deletion gives rise to a seizure phenotype with many of the features seen in rodent models of focal temporal lobe epilepsy (TLE) – e.g., with kainic acid administration (Lothman and Collins, 1981; Schwartzkroin, 1994). Further, the TLE-like seizure pattern in Kv1.1 knock-out mice gives rise to pathological changes characteristic of TLE - cell loss in hippocampal subfields and dentate hilus, mossy fiber reorganization, and reactive astrogliosis. These neuropathological features also resemble those seen in kainic acid and pilocarpine rodent models (Bouilleret et al., 1999; McKhann et al., 2003; Dudek, 2006) as well as in human temporal lobe from TLE patients (Sutula et al., 1989; Franck et al., 1995; Houser, 1999). Holmes and Ben-Ari (2003) have made the case that experimental tests of novel therapies should be conducted in models that exhibit pathologies similar to those patients to be treated clinically (i.e., not on “normal” brains). In many respects, the Kv1.1 mouse offers such a model system for our gene transfer study – including the considerable animal-to-animal variability observed with respect to severity of the seizure

phenotype. To deal with this variability, one must be able to assess a relatively large population of animals, and assess not only with the gene of interest (in our case, *Kcna1*), but also "innocuous" genes (such as a reporter gene) that control for effects of the injection procedure. In addition, the treatment protocol must be developed with sensitivity to the "natural history" of seizure activity in the model, so that treatment efforts can be assessed against the expected levels of activity – developmentally, diurnally, etc.

Seizures typically begin to appear in Kv1.1 knock-out mice during the third postnatal week - well before we can identify any neuropathology characteristic of TLE. In our hands, the latter appeared only after animals had experienced weeks (or months) of spontaneous seizure activity – and significant neuropathology was seen only in animals exhibiting prolonged, severe seizure episodes (i.e., status epilepticus). Our limited EEG recordings provide preliminary support for the notion that seizure activity is initiated focally, in the temporal lobe/hippocampus; however, our current data are too limited to support a concrete conclusion on this issue. These observations in the Kv1.1 knock-out mouse are consistent with the view that, at least in some types of TLE, there is a generalized (not focal) genetic (or other?) disturbance that is expressed as a focal seizure disorder. According to this hypothesis, focal hippocampal pathology is not the "cause" of the chronic seizure activity; rather, focal abnormalities reflect the consequences of seizure activity in particularly sensitive cell populations (e.g., as has been shown earlier for the *stargazer* mutant mouse in developing TLE-like pathology (Qiao &Noebels, 1993)).

A number of clinical reports have identified *Kcna1* dysfunction/loss as a contributor to epileptogenicity and hyperexcitability in human brain (Browne et al., 1994; Scheffer et al., 1998; Zuberi et al., 1999; Eunson et al., 2000). Further, as indicated above, another mouse mutation (*mceph*/*mceph*) with widespread expression of abnormal gene product has a phenotypic expression of partial complex seizures (Persson et al., 2005). A recent study has also shown that Kv1-containing channels are tightly associated with Lgi1 (the protein product of the *leucine-rich glioma inactivator gene1* (*LGI1*)) (Schulte et al., 2006). Mutation of *LGI1* has been reported as the causative basis for an autosomal dominant form of lateral temporal lobe epilepsy (ADLTE), characterized by partial seizures and auditory features (Morante-Redolat et al., 2002; Ottman et al., 2004). Strong expression of Kv1.1 and Kv1.2 in auditory brainstem neurons (Grigg et al., 2000) and their role in auditory signal encoding (Brew et al., 2003) provide a speculative link between *LGI1*-related seizure activity and the auditory phenotype. In the hippocampus, the Lgi1 expression pattern partially overlaps with Kv1.1 localization (Schulte et al., 2006). Lesioning and inactivation experiments, in which Lgi1 mutation selectively abolished Kvβ1-mediated inactivation in Kv channels assembled from Kv1.1, Kv1.4 and Kvβ1 subunits, suggest that both Kv1.1 and Lgi1 are co-assembled with Kv1.4 and Kvβ1 in axonal terminals (Schulte et al., 2006). The removal of Kvβ1-mediated Lig1 inactivation in presynaptic A-type channels would result in modulation of A-type K^+currents in hippocampal excitatory synapses, leading to focal hyperexcitability (epileptogenesis) in the temporal lobe (Schulte et al., 2006).

While the *Kcna1*gene is normally expressed throughout the brain, there are some regions of particularly high expression - including hippocampal subfields - often thought to be involved in common seizure types (e.g., TLE). The model therefore gives us an opportunity to test the idea that focal treatment – indeed, treatment of a specific cell population – can reduce a generalized functional pathology expressed as seizure activity. The data summarized in the above paragraph are consistent with the idea that a focal dysfunction may arise from the generalized loss of a channel subunit, especially when there is a focal co-expression (or co-assembly) of that protein with other proteins/subunits involved in normal channel function. As a result, loss of axonal/terminal A-type potassium currents - a product of Kv1.1 and Kv1.4 co-assembly with other closely associated proteins such as Lgi1 and Kvβ1 – might lead to TLE-

like seizure phenotypes in both autosomal dominant lateral TLE in human and Kv1.1 knock-out in mice.

Viral vector-mediated Kv1.1 gene transfer

Vector-mediated gene transfer has become an attractive choice for both basic neurobiological investigations and CNS gene therapy (Sapolsky, 2003; Vezzani, 2004; McCown, 2005; Deglon and Hantraye, 2005). Since approximately 30% of epilepsy patients are refractory to conventional antiepileptic drug treatment (Kwan and Brodie, 2000), novel approaches to therapy are needed. Although still unproven, gene therapy might provide an alternative treatment option (McCown, 2004). Various viral vectors, including herpes simplex virus, adenoviruses and retroviruses have been developed and modified to introduce foreign cDNAs into CNS cells; these exogenously introduced genes, in turn, give rise to expression of specific proteins (e.g., transmitters, growth factors, ion channels) to influence and/or cure CNS diseases (Montain, 2000; Glorioso and Fink, 2004; McCown, 2005; Deglon and Hantraye, 2005; Verma and Weitzman, 2005).

To date, most such studies focusing epileptic conditions have adopted a strategy of introducing, or up-regulating, a protein known to be generally inhibitory – but not necessarily linked to the specific genetic defect thought to give rise to the epilepsy or brain hyperexcitability. In the current study, we have taken a somewhat different tack. We have taken advantage of a model in which a known gene deletion gives rise to epilepsy, and attempted to “restore” the normal gene by delivering it locally - by viral vector-mediated gene transfer - into a specific (restricted) neuronal population thought to be critical to the initiation of seizure activity. Our long-term goal is to express the gene of interest, *Kcna1*, so as to influence (i.e., block) seizure activity (e.g., see Simonato et al., 2000). Our gene delivery strategy was based on a previous study, in which *overexpression* of *Kcna1* (in a genetically normal mouse) via the same HSV1 vector was shown to provide neuroprotection against kainic acid-induced seizures (Lee et al. 2003). The vector uses an amplicon-based bipromotor system which permits expression of both the gene of interest and a reporter gene (Yenari and Sapolsky, 2005). Therefore, one can demonstrate the successful infection of cells by observing the product of the reporter gene.

In hindsight, there are certainly a number of negative features associated with our strategy and choice of vector. For example, because the reporter gene is under independent promoter control, it is possible for the infected cell to express the reporter gene but not (or to a much lesser extent) the gene of interest – in our case, the gene for the Kv1.1 α subunit. The results of our Kv1.1 immunostaining suggest that this selective expression did in fact occur, since high levels of β-gal (shown in X-gal reacted material) were seen in many neurons but Kv1.1 immunoreactivity was seen in a much smaller cell population. This result was somewhat surprising given the previous observation of ~98% co-expression (Fink et al., 1997) of this combination of marker and transgenes. It is possible that the difference observed is due to the sensitivities of the different methods of detection used: a histochemical reaction for β-gal and immunocytochemistry for Kcna1. Indeed, when ICC (rather than a histochemical technique) was used to detect β-gal, there was a comparable pattern of staining for both Kcna1 and the marker protein. Still, the potential for “independent” expression could be better addressed by fusing the marker gene (or an immunohistochemically-recognizable epitope) to the gene of interest, so that gene transcription results in both products.

Other noteworthy features of the HSV1 vector used in these studies include its neuronal specificity (no glia were infected) and its apparent preference for infecting hippocampal granule cells (Ho et al., 1995). The specificity of a particular vector for a given cell type may be particularly useful if one plans to target that cell population with the exogenous gene. The granule cells appear to be a good target in the Kv1.1 knockout mouse, since mossy fibers normally express the Kv1.1 subunit at relatively high levels. Other cell types, such as CA3

pyramidal cells and various interneuron sub-populations also normally express Kv1.1 – so it remains unclear if preferentially providing a single cell population with the exogenous gene is an effective way to reduce hyperexcitability that results from general Kv1.1 deletion. Especially given the widespread expression of Kv1.1 channels in other cortical brain regions, is it important for the vector to be introduced widely (e.g., including neocortex) to have significant functional consequences? Other vector systems are likely to have different (or less specific) cell preferences (Wong et al., 2005; Janas et al., 2006). Determining the need for general vs. cell-specific infection is an important prerequisite for this gene therapy approach, and studies of vectors with differential targeting capabilities should provide valuable information about this question.

It is important to note that in those cells (granule and CA3 pyramidal cells) successfully infected, the Kv1.1 α subunit was not localized to the appropriate (i.e., normally occurring) subcellular compartment. Although this observation may reflect an immature subunit localization due to the relatively short period between vector injection and host animal sacrifice (typically 3-6 days), these results are consistent with analyses of subcellular trafficking of Kv1.1-containing channels in heterologous cells and cultured hippocampal neurons (Manganas et al., 2000; 2001). Channels formed from Kv1.1 subunits alone (i.e., homomeric Kv1.1 channels) are inefficiently trafficked to the plasma membrane from their site of assembly in the endoplasmic reticulum, where they accumulate. Acute ectopic expression of high (non-stoichiometric) levels of *Kcna1*, on the Kv1.1$^{-/-}$ background, may result in assembly of such homomeric Kv1.1 channels (not normally found in the brain) and inefficient trafficking to axons. Normal localization of subunits from exogenous gene expression remains an important goal of our research. Such localization may be facilitated by co-expression of Kv1.1 with other component subunits of native Kv1.1-containing complexes (e.g., Kv1.4, Kvβ2), or by expression of mutant Kv1.1 isoforms with enhanced surface expression (Manganas et al., 2001). The degree to which normal vs. ectopic subunit expression influences cell excitability remains to be tested.

Finally, it is well known that HSV amplicons express for only a few days (Ho et al., 1995) – i.e., the HSV1 – Kv1.1 vector system appears to be relatively unstable in its infection/gene expression efficacy. Such a system may well be sub-optimal for studying an animal in which gene deletion produces a *chronic* hyperexcitability disorder. At the very least, one must be able to examine the epileptic phenotype of the Kv1.1 knockout mouse (i.e., carry out EEG monitoring) during a time window in which the vector-mediated gene expression is likely to provide the proteins of interest. While HSV1 gene expression capability is limited to a few days, more pertinent questions are: How long does it take to get the protein to its functional destination? And How long does the gene product lasts (what is the turnover rate of channel protein)? These questions must still be addressed – if not with the HSV1 system, then with other vector (or other gene transfer) systems.

Can gene transfer (e.g., into dentate granule cells or hippocampal CA3 pyramidal neurons) actually reduce brain excitability? Previous studies with recombinant adeno-associated virus (rAAV) vectors have shown that gene transfer can modulate seizure activities. For example, expression (and subsequent secretion) of the neuroactive peptide, galanin, was shown to attenuate both focal seizure activity and seizure-induced cell death (Haberman et al., 2003). In addition, overexpression of neuropeptide Y (NPY) in hippocampal neurons affords functionally significant protection from limbic seizures (including status epilepticus) and retards kindling (Richichi et al., 2004). The AAV vector expresses for weeks, thus providing the potential for long-lasting overexpression of a transgene of interest. Given the apparent success of AAV vector experiments, it is worth noting that 80% of the human population tests positive for antibodies to wild-type AAV2 protein, a condition that could neutralize the efficacy and increase the likelihood of inflammation with CNS transfection via AAV (Peden et al.,

2004; McCown, 2004) in the clinical setting. Such issues must also be considered in the development of optimal vector systems if gene therapy approaches are to be applied at the clinical level.

Even given an effective vector system, the efficacy of gene transfer in modulating (curing?) a chronic, genetically-based epilepsy is uncertain. Is gene transfer into an animal with a long-established epilepsy simply too late? Perhaps once seizure activity is established, and there are consequent alterations in brain circuitry, the insertion of exogenous replacement (or inhibitory) channels is unlikely to be therapeutic. Gene expression at an inappropriate time point in development, or vector transcription that is not coordinated with that of other related endogenous genes, may give rise to channel sub-types and locations that further unbalance the system. In short, one might argue that insertion of exogenous channel protein (and generation of non-native channels) into developmentally “deprived” networks cannot make them normal. The evidence to date is inadequate for drawing a conclusion. The potential power of this molecular/genetic approach, however, encourages further experimentation targeted to specific aspects of this complex question.

Acknowledgements

This study was funded by a Grant Award from Citizens United for Research in Epilepsy (CURE) (PAS), and by NIH grants DC002739 (BLT) and NS034383 (JST). We are grateful to K. Katleba, C.A. Robbins and Dr. M. Wenzel for excellence in technical support.

References

Almgren M, Persson AS, Fenghua C, Witgen BM, Schalling M, Nyengaard JR, Lavebratt C. Lack of potassium channel induces proliferation and survival causing increased neurogenesis and two-fold hippocampus enlargement. Hippocampus. 2007DOI 10.1002/hipo.20268

Baraban SC, Hollopeter G, Erickson JC, Schwartzkroin PA, Palmiter RD. Knock-out mice reveal a critical antiepileptic role for neuropeptide Y. J Neurosci 1997;17:8927–8936. [PubMed: 9364040]

Bouilleret V, Ridoux V, Depaulis A, Marescaux C, Nehlig A, Le Gal La Salle G. Recurrent seizures and hippocampal sclerosis following intrahippocampal kainate injection in adult mice: electroencephalography, histopathology and synaptic reorganization similar to mesial temporal lobe epilepsy. Neuroscience 1999;89:717–729. [PubMed: 10199607]

Brew HM, Hallows JL, Tempel BL. Hyperexcitability and reduced low threshold potassium currents in auditory neurons of mice lacking the voltage-gated potassium channel subunit Kv1.1. J Physiol (London) 2003;458:1–20. [PubMed: 12611922]

Browne DL, Gancher ST, Nutt JG, Brunt ER, Smith EA, Kramer P, Litt M. Episodic ataxia/myokymia syndrome is associated with point mutations in the human potassium channel gene, KCNA1. Nat Genet 1994;8:136–140. [PubMed: 7842011]

Burgess, DL. Transgenic and gene replacement models of epilepsy:Targeting ion channel and neurotransmission pathways in mice.. In: Pitkanen, A.; Schwartzkroin, PA.; Moshe, SL., editors. Models of Seizures and Epilepsy. Elsevier Academic Press; San Diego: 2006. p. 199-222.

Burgess DL, Noebels JL. Voltage-dependent calcium channel mutations in neurological disease. Ann N Y Acad Sci 1999;868:199–212. [PubMed: 10414295]

Cavalheiro, EA.; Naffah-Mazzacoratti, MG.; Mello, LE.; Leite, JP. The pilocarpine model of seizures.. In: Pitkanen, A.; Schwartzkroin, PA.; Moshe, SL., editors. Models of Seizures and Epilepsy. Elsevier Academic Press; San Diego: 2006. p. 433-448.

Chen Q, He Y, Yang K. Gene therapy for Parkinson's disease: progress and challenges. Curr Gene Ther 2005;5:71–80. [PubMed: 15638712]

Christensen JK, Paternain AV, Selak S, Ahring PK, Lerma J. A mosaic of functional kainate receptors in hippocampal interneurons. J Neurosci 2004;24:8986–8993. [PubMed: 15483117]

Coleman SK, Newcombe J, Pryke J, Dolly JO. Subunit composition of Kv1 channels in human CNS. J Neurochem 1999;73:849–858. [PubMed: 10428084]

Cooper EC, Milroy A, Jan YN, Jan LY, Lowenstein DH. Presynaptic localization of Kv1.4-containing A-type potassium channels near excitatory synapses in the hippocampus. J Neurosci 1998;18:965–974. [PubMed: 9437018]

Deglon N, Hantraye P. Viral vectors as tools to model and treat neurodegenerative disorders. J Gene Med 2005;7:530–539. [PubMed: 15651039]

Dodson PD, Forsythe ID. Presynaptic K+ channels: electrifying regulators of synaptic terminal excitability. Trends Neurosci 2004;27:210–217. [PubMed: 15046880]

Donahue LR, Cook SA, Johnson KR, Bronson RT, Davisson MT. Megencephaly: a new mouse mutation on chromosome 6 that causes hypertrophy of the brain. Mamm Genome 1996;7:871–876. [PubMed: 8995755]

Dudek, FE.; Clark, S.; Williams, PA.; Grabenstatter, H. Kainate-induced status epilepticus: A chronic model of acquired epilepsy.. In: Pitkanen, A.; Schwartzkroin, PA.; Moshe, SL., editors. Models of Seizures and Epilepsy. Vol. 1 edn. Elsevier Academic Press; San Diego: 2006. p. 415-432.

Dumas T, McLaughlin J, Ho D, Meier T, Sapolsky R. Delivery of herpes simplex virus amplicon-based vectors to the dentate gyrus does not alter hippocampal synaptic transmission in vivo. Gene Ther 1999;6:1679–1684. [PubMed: 10516716]

Eunson LH, Rea R, Zuberi SM, Youroukos S, Panayiotopoulos CP, Kiguori R, Avoni P, McWilliam RC, Stephenson JB, Janna MG, Kullmann DM, Spauschus A. Clinical, genetic, and expression studies of mutations in the potassium channel gene KCNA1 reveal new pehotypic variability. Ann Neurol 2000;48:647–656. [PubMed: 11026449]

Fink SL, Chang L, Ho D, Sapolsky R. Defective herpes simplex virus vectors expressing the rat brain stress-inducible heat shock protein 72 protect cultured neurons from severe heat shock. J Neurochem 1997;68:961–969. [PubMed: 9048741]

Fisher RS, Ho J. Potential new methods for antiepileptic drug delivery. CNS Drugs 2002;16:579–593. [PubMed: 12153331]

Frampton AR Jr. Goins WF, Nakano K, Burton EA, Glorioso JC. HSV trafficking and development of gene therapy vectors with applications in the nervous system. Gene Ther 2005;12:891–901. [PubMed: 15908995]

Franck JE, Pokorny J, Kunkel DD, Schwartzkroin PA. Physiologic and morphologic characteristics of granule cell circuitry in human epileptic hippocampus. Epilepsia 1995;36:543–558. [PubMed: 7555966]

Franklin, KBJ.; Paxinos, GT. The mouse brain in stereotaxic coordinates. Academic Press; San Diego: 1997.

Geiger JR, Jonas P. Dynamic control of presynaptic Ca(2+) inflow by fast-inactivating K(+) channels in hippocampal mossy fiber boutons. Neuron 2000;28:927–939. [PubMed: 11163277]

Gittelman JX, Tempel BL. Kv1.1-containing channels are critical for temporal precision during spike initiation. J Neurophysiol 2006;96:1203–1214. [PubMed: 16672305]

Glorioso JC, Fink DJ. Herpes vector-mediated gene transfer in treatment of diseases of the nervous system. Annu Rev Microbiol 2004;58:253–271. [PubMed: 15487938]

Grigg JJ, Brew HM, Tempel BL. Expression of voltage-gated potassium channel genes in auditory nuclei of the mouse brainstem. Hearing Res 2000;140:77–90.

Grosse G, Draguhn A, Hohne L, Tapp R, Veh RW, Ahnert-Hilger G. J Neurosci 2000;20:1869–1882. [PubMed: 10684888]

Gundersen HJ, Jensen EB. The efficiency of systematic sampling in stereology and its prediction. J Microsc 1987;147:229–263. [PubMed: 3430576]

Haberman RP, Samulski RJ, McCown TJ. Attenuation of seizures and neuronal death by adeno-associated virus vector galanin expression and secretion. Nat Med 2003;9:1076–1080. [PubMed: 12858168]

Hallows JL, Tempel BL. Expression of Kv1.1, a Shaker-like potassium channel, is temporally regulated in embryonic neurons and glia. J Neurosci 1998;18:5682–5691. [PubMed: 9671659]

Ho DY, Fink S, Lawrence M, Meier T, Saydam T, Dash R, Sapolsky R. Herpes simplex virus vector system: Analysis of its in vivo and in vitro cytopathic effects. J Neurosci Meth 1995;57:205–215.

Holmes GL, Ben-Ari Y. Seizing hold of seizures. Nat Med 2003;9:994–996. [PubMed: 12894158]

Houser CR. Neuronal loss and synaptic reorganization in temporal lobe epilepsy. Adv Neurol 1999;79:743–761. [PubMed: 10514861]

Hsu SM, Raine L, Fanger H. Use of avidin-biotin-peroxidase complex (ABC) in immunoperoxidase techniques: a comparison between ABC and unlabeled antibody (PAP) procedures. J Histochem Cytochem 1981;29:577–580. [PubMed: 6166661]

Inchauspe CG, Martini FJ, Forsythe ID, Uchitel OD. Functional compensation of P/Q by N-type channels blocks short-term plasticity at the calyx of Held presynaptic terminal. J Neurosci 2004;24:10379–10383. [PubMed: 15548652]

Janas J, Skowronski J, Van Aelst L. Lentiviral delivery of RNAi in hippocampal neurons. Methods Enzymol 2006;406:593–605. [PubMed: 16472690]

Kaminski JM, Nguyen K, Buyyounouski M, Pollack A. Prostate cancer gene therapy and the role of radiation. Cancer Treat Rev 2002;28:49–64. [PubMed: 12027414]

Koch RO, Wanner SG, Koschak A, Hanner M, Schwarzer C, Kaczorowski GJ, Slaughter RS, Garcia ML, Knaus HG. Complex subunit assembly of neuronal voltage-gated K+ channels. Basis for high-affinity toxin interactions and pharmacology. J Biol Chem 1997;272:27577–27581. [PubMed: 9346893]

Kwan P, Brodie MJ. Early identification of refractory epilepsy. N Engl J Med 2000;342:314–319. [PubMed: 10660394]

Lee AL, Dumas TC, Tarapore PE, Webster BR, Ho DY, Kaufer D, Sapolsky RM. Potassium channel gene therapy can prevent neuron death resulting from necrotic and apoptotic insults. J Neurochem 2003;86:1079–1088. [PubMed: 12911616]

Lin EJ, Richichi C, Young D, Baer K, Vezzani A, During MJ. Recombinant AAV-mediated expression of galanin in rat hippocampus suppresses seizure development. Eur J Neurosci 2003;18:2087–2092. [PubMed: 14622242]

Liu H, Kaur J, Dashtipour K, Kinyamu R, Ribak CE, Friedman LK. Suppression of hippocampal neurogenesis is associated with developmental stage, number of perinatal seizure episodes, and glucocorticosteroid level. Exp Neurol 2003;184:196–213. [PubMed: 14637092]

Lopantsev V, Tempel BL, Schwartzkroin PA. Hyperexcitability of CA3 pyramidal cells in mice lacking the potassium channel subunit Kv1.1. Epilepsia 2003;44:1506–1512. [PubMed: 14636320]

Lothman EW, Collins RC. Kainic acid induced limbic seizures: metabolic, behavioral, electroencephalographic and neuropathological correlates. Brain Res 1981;218:299–318. [PubMed: 7272738]

Manganas LN, Trimmer JS. Subunit composition determines Kv1 potassium channel surface expression. J Biol Chem 2000;275:29685–29693. [PubMed: 10896669]

Maganas LN, Wang Q, Scannevin RH, Antonucci DE, Rhodes KJ, Trimmer JS. Indentification of a trafficking determinant localized to the Kv1 potassium channel pore. Proc Natl Acad Sci USA 2001;98:14055–14059. [PubMed: 11698661]

Mazarati A, Wasterlain CG. Anticonvulsant effects of four neuropeptides in the rat hippocampus during self-sustaining status epilepticus. Neurosci Lett 2002;331:123–127. [PubMed: 12361856]

Mazarati A, Langel U, Bartfai T. Galanin: an endogenous anticonvulsant? Neuroscientist 2001;7:506–517. [PubMed: 11765128]

McCown TJ. The clinical potential of antiepileptic gene therapy. Expert Opin Biol Ther 2004;4:1771–1776. [PubMed: 15500405]

McCown TJ. Adeno-associated virus (AAV) vectors in the CNS. Curr Gene Ther 2005;5:333–338. [PubMed: 15975010]

McKhann GM 2nd, Wenzel HJ, Robbins CA, Sosunov AA, Schwartzkroin PA. Mouse strain differences in kainic acid sensitivity, seizure behavior, mortality, and hippocampal pathology. Neuroscience 2003;122:551–561. [PubMed: 14614919]

Menegola M, Trimmer JS. Unanticipated region- and cell-specific downregulation of individual KChIP auxiliary subunit isotypes in Kv4.2 knockout mouse brain. J Neurosci 2006;26:12137–12142. [PubMed: 17122038]

Monaghan MM, Trimmer JS, Rhodes KJ. Experimental localization of Kv1 family voltage-gated K+ channel alpha and beta subunits in rat hippocampal formation. J Neurosci 2001;21:5973–5983. [PubMed: 11487620]

Morante-Redolat JM, Gorostidi-Pagola A, Piquer-Sirerol S, Saenz A, Poza JJ, Galan J, Gesk S, Sarafidou T, Mautner VF, Binelli S, Staub E, Hinzmann B, French L, Prud'homme JF, Passarelli D, Scannapieco P, Tassinari CA, Avanzini G, Marti-Masso JF, Kluwe L, Deloukas P, Moschonas NK, Michelucci R, Siebert R, Nobile C, Perez-Tur J, Lopez de Munain A. Mutations in the LGI1/Epitempin gene on 10q24 cause autosomal dominant lateral temporal epilepsy. Hum Mol Genet 2002;11:1119–1128. [PubMed: 11978770]

Mountain A. Gene therapy: the first decade. Trends Biotechnol 2000;18:119–128. [PubMed: 10675899]

Mulley JC, Scheffer IE, Petrou S, Berkovic SF. Channelopathies as a genetic cause of epilepsy. Curr Opin Neurol 2003;16:171–176. [PubMed: 12644745]

Noebels JL. The biology of epilepsy genes. Annu Rev Neurosci 2003;26:599–625. [PubMed: 14527270]

Noebels, JL. Spontaneous epileptic mutations in the mouse.. In: Pitkanen, A.; Schwartzkroin, PA.; Moshe, SL., editors. Models of Seizures and Epilepsy. Vol. 1 edn. Elsevier Academic Press; San Diego: 2006. p. 223-232.

O'Grady SM, Lee SY. Molecular diversity and function of voltage-gated (Kv) potassium channels in epithelial cells. Int J Biochem Cell Biol 2005;37:1578–1594. [PubMed: 15882958]

Ogris W, Lehner R, Fuchs K, Furtmuller B, Hoger H, Homanics GE, Sieghart W. Investigation of the abundance and subunit composition of GABAA receptor subtypes in the cerebellum of alpha1-subunit-deficient mice. J Neurochem 2006;96:136–147. [PubMed: 16277610]

Ottman R, Winawer MR, Kalachikov S, Barker-Cummings C, Gilliam TC, Pedley TA, Hauser WA. LGI1 mutations in autosomal dominant partial epilepsy with auditory features. Neurology 2004;62:1120–1126. [PubMed: 15079011]

Papazian DM, Schwarz TL, Tempel BL, Jan YN, Jan LY. Cloning of genomic and complementary DNA from Shaker, a putative potassium channel gene from Drosophila. Science 1987;237:749–753. [PubMed: 2441470]

Peden CS, Burger C, Muzyczka N, Mandel RJ. Circulating anti-wild-type adeno-associated virus type 2 (AAV2) antibodies inhibit recombinant AAV2 (rAAV2)-mediated, but not rAAV5-mediated, gene transfer in the brain. J Virol 2004;78:6344–6359. [PubMed: 15163728]

Persson AS, Westman E, Want FH, Khan FH, Spenger C, Lavebratt C. Kv1.1 nulll mice have enlarged hippocampus and ventral cortex. BMC Neurosci. 2007doi:10.1186/1471-2202-8-10

Persson AS, Klement G, Almgren M, Sahlholm K, Nilsson J, Petersson S, Arhem P, Schalling M, Lavebratt C. A truncated Kv1.1 protein in the brain of the megencephaly mouse: expression and interaction. BMC Neurosci 2005;6:65. [PubMed: 16305740]

Petersson S, Persson AS, Johansen JE, Ingvar M, Nilsson J, Klement G, Arhem P, Schalling M, Lavebratt C. Truncation of the Shaker-like voltage-gated potassium channel, Kv1.1, causes megencephaly. Eur J Neurosci 2003;18:3231–3240. [PubMed: 14686897]

Qiao X, Noebels JL. Developmental analysis of hippocampal mossy fiber outgrowth in a mutant mouse with inherited spike-wave seizures. J Neurosci 1993;13:4622–4635. [PubMed: 8229188]

Rettig J, Heinemann SH, Wunder F, Lorra C, Parcej DN, Dolly JO, Pongs O. Inactivation properties of voltage-gated K+ channels altered by presence of beta-subunit. Nature 1994;369:289–294. [PubMed: 8183366]

Rho JM, Szot P, Tempel BL, Schwartzkroin PA. Developmental seizure susceptibility of kv1.1 potassium channel knockout mice. Dev Neurosci 1999;21:320–327. [PubMed: 10575255]

Rhodes KJ, Keilbaugh SA, Barrezueta NX, Lopez KL, Trimmer JS. Association and colocalization of K + channel alpha- and beta-subunit polypeptides in rat brain. J Neurosci 1995;15:5360–5371. [PubMed: 7623158]

Rhodes KJ, Strassle BW, Monaghan MM, Bekele-Arcuri Z, Matos MF, Trimmer JS. Association and colocalization of the Kvbeta1 and Kvbeta2 beta-subunits with Kv1 alpha-subunits in mammalian brain K+ channel complexes. J Neurosci 1997;17:8246–8258. [PubMed: 9334400]

Richichi C, Lin EJ, Stefanin D, Colella D, Ravizza T, Grignaschi G, Veglianese P, Sperk G, During MJ, Vezzani A. Anticonvulsant and antiepileptogenic effects mediated by adeno-associated virus vector neuropeptide Y expression in the rat hippocampus. J Neurosci 2004;24:3051–3059. [PubMed: 15044544]

Ruppersberg JP, Schroter KH, Sakmann B, Stocker M, Sewing S, Pongs O. Heteromultimeric channels formed by rat brain potassium-channel proteins. Nature 1990;345:535–537. [PubMed: 2348860]

Sapolsky R. Neuroprotective gene therapy. Nat Rev Neurosci 2003;4:61–69. [PubMed: 12511862]

Scheffer H, Brunt ER, Mol GJ, van der Vlies P, Stulp RP, Verlind E, Mantel G, Averyanov YN, Hofstra RM, Buys CH. Three novel KCNA1 mutations in episodic ataxia type I families. Hum Genet 1998;102:464–466. [PubMed: 9600245]

Schulte U, Thumfart JO, Klocker N, Sailer CA, Bildl W, Biniossek M, Dehn D, Deller T, Eble S, Abbass K, Wangler T, Knaus HG, Fakler B. The epilepsy-linked Lgi1 protein assembles into presynaptic Kv1 channels and inhibits inactivation by Kvbeta1. Neuron 2006;49:697–706. [PubMed: 16504945]

Schwartzkroin PA. Cellular electrophysiology of human epilepsy. Epilepsy Res 1994;17:185–192. [PubMed: 8013442]

Shamotienko OG, Parcej DN, Dolly JO. Subunit combinations defined for K+ channel Kv1 subtypes in synaptic membrances from bovine brain. Biochem 1997;36:8195–8201. [PubMed: 9204863]

Sheng M, Tsaur ML, Jan YN, Jan LY. Subcellular segregation of two A-type K+ channel proteins in rat central neurons. Neuron 1992;9:271–284. [PubMed: 1497894]

Sheng M, Liao YJ, Jan YN, Jan LY. Presynaptic A-current based on heteromultimeric K+ channels detected in vivo. Nature 1993;365:72–75. [PubMed: 8361540]

Shieh CC, Coghlan M, Sullivan JP, Gopalakrishnan M. Potassium channels: molecular defects, diseases, and therapeutic opportunities. Pharmacol Rev 2000;52:557–594. [PubMed: 11121510]

Simonato M, Manservigi R, Marconi P, Glorioso J. Gene transfer into neurones for the molecular analysis of behaviour: focus on herpes simplex vectors. Trends Neurosci 2000;23:183–190. [PubMed: 10782119]

Smart SL, Lopantsev V, Zhang CL, Robbins CA, Wang H, Chiu SY, Schwartzkroin PA, Messing A, Tempel BL. Deletion of the K(V)1.1 potassium channel causes epilepsy in mice. Neuron 1998;20:809–819. [PubMed: 9581771]

Steinlein OK, Noebels JL. Ion channels and epilepsy in man and mouse. Curr Opin Genet Dev 2000;10:286–291. [PubMed: 10826987]

Strassle BW, Menegola M, Rhodes KJ, Trimmer JS. Light and electron microscopic analysis of KChIP and Kv4 localization in rat cerebellar granule cells. J Comp Neurol 2005;484:144–155. [PubMed: 15736227]

Stuhmer W, Stocker M, Sakmann B, Seeburg P, Baumann A, Grupe A, Pongs O. Potassium channels expressed from rat brain cDNA have delayed rectifier properties. FEBS Lett 1988;242:199–206. [PubMed: 2462513]

Sutula T, Cascino G, Cavazos J, Parada I, Ramirez L. Mossy fiber synaptic reorganization in the epileptic human temporal lobe. Ann Neurol 1989;26:321–330. [PubMed: 2508534]

Tauck DL, Nadler JV. Evidence of functional mossy fiber sprouting in hippocampal formation of kainic acid-treated rats. J Neurosci 1985;5:1016–1022. [PubMed: 3981241]

Tempel BL, Jan YN, Jan LY. Cloning of a probable potassium channel gene from mouse brain. Nature 1988;332:837–839. [PubMed: 2451788]

Trimmer JS. Immunological identification and characterization of a delayed rectifier K+ channel polypeptide in rat brain. Proc Natl Acad Sci USA 1991;88:10764–10768. [PubMed: 1961744]

Trimmer JS. Regulation of ion channel expression by cytoplasmic subunits. Curr Opin Neurobiol 1998;8:370–374. [PubMed: 9687351]

Trimmer JS, Rhodes KJ. Localization of voltage-gated ion channels in mammalian brain. Annu Rev Physiol 2004;66:477–519. [PubMed: 14977411]

Vadolas J, Williamson R, Ioannou PA. Gene therapy for inherited lung disorders: an insight into pulmonary defence. Pulm Pharmacol Ther 2002;15:61–72. [PubMed: 11969364]

Verma IM, Weitzman MD. Gene therapy: twenty-first century medicine. Annu Rev Biochem 2005;74:711–738. [PubMed: 15952901]

Vezzani A, Sperk G. Overexpression of NPY and Y2 receptors in epileptic brain tissue: an endogenous neuroprotective mechanism in temporal lobe epilepsy? Neuropeptides 2004;38:245–252. [PubMed: 15337376]

Wang H, Kunkel DD, Schwartzkroin PA, Tempel BL. Localization of Kv1.1 and Kv1.2, two K channel proteins, to synaptic terminals, somata, and dendrites in the mouse brain. J Neurosci 1994;14:4588–4599. [PubMed: 8046438]

Wang H, Kunkel DD, Martin TM, Schwartzkroin PA, Tempel BL. Heteromultimeric K+ channels in terminal and juxtaparanodal regions of neurons. Nature 1993;365:75–79. [PubMed: 8361541]

Welsh N. Gene therapy in diabetes mellitus: promises and piffalls. Curr Opin Mol Ther 1999;1:464–470. [PubMed: 11713761]

Wenzel HJ, Robbins CA, Tsai LH, Schwartzkroin PA. Abnormal morphological and functional organization of the hippocampus in a p35 mutant model of cortical dysplasia associated with spontaneous seizures. J Neurosci 2001;21:983–998. [PubMed: 11157084]

Wenzel HJ, Patel LS, Robbins CA, Emmi A, Yeung RS, Schwartzkroin PA. Morphology of cerebral lesions in the Eker rat model of tuberous sclerosis. Acta Neuropathol (Berl) 2004;108:97–108. [PubMed: 15185103]

West MJ, Slomianka L, Gundersen HJ. Unbiased stereological estimation of the total number of neurons in the subdivisions of the rat hippocampus using the optical fractionator. Anat Rec 1991;231:482–497. [PubMed: 1793176]

Wong LF, Ralph GS, Walmsley LE, Bienemann AS, Parham S, Kingsman SM, Uney JB, Mazarakis ND. Lentiviral-mediated delivery of Bcl-2 or GDNF protects against excitotoxicity in the rat hippocampus. Mol Ther 2005;11:89–95. [PubMed: 15585409]

Yang Y, Frankel WN. Genetic approaches to studying mouse models of human seizure disorders. Adv Exp Med Biol 2004;548:1–11. [PubMed: 15250582]

Yenari MA, Sapolsky RM. Gene therapy in neurological disease. Methods Mol Med 2005;104:75–88. [PubMed: 15454665]

Zhao X, Ahram A, Berman RF, Muizelaar JP, Lyeth BG. Early loss of astrocytes after experimental traumatic brain injury. Glia 2003;44:140–152. [PubMed: 14515330]

Zuberi SM, Eunson LH, Spauschus A, De Silva R, Tolmie J, Wood NW, McWilliam RC, Stephenson JP, Kullmann DM, Hanna MG. A novel mutation in the human voltate-gated potassium channel gene (Kv1.1) associates with episodic ataxia type I and sometimes with partial epilepsy. Brain 1999;122:817–825. [PubMed: 10355668]

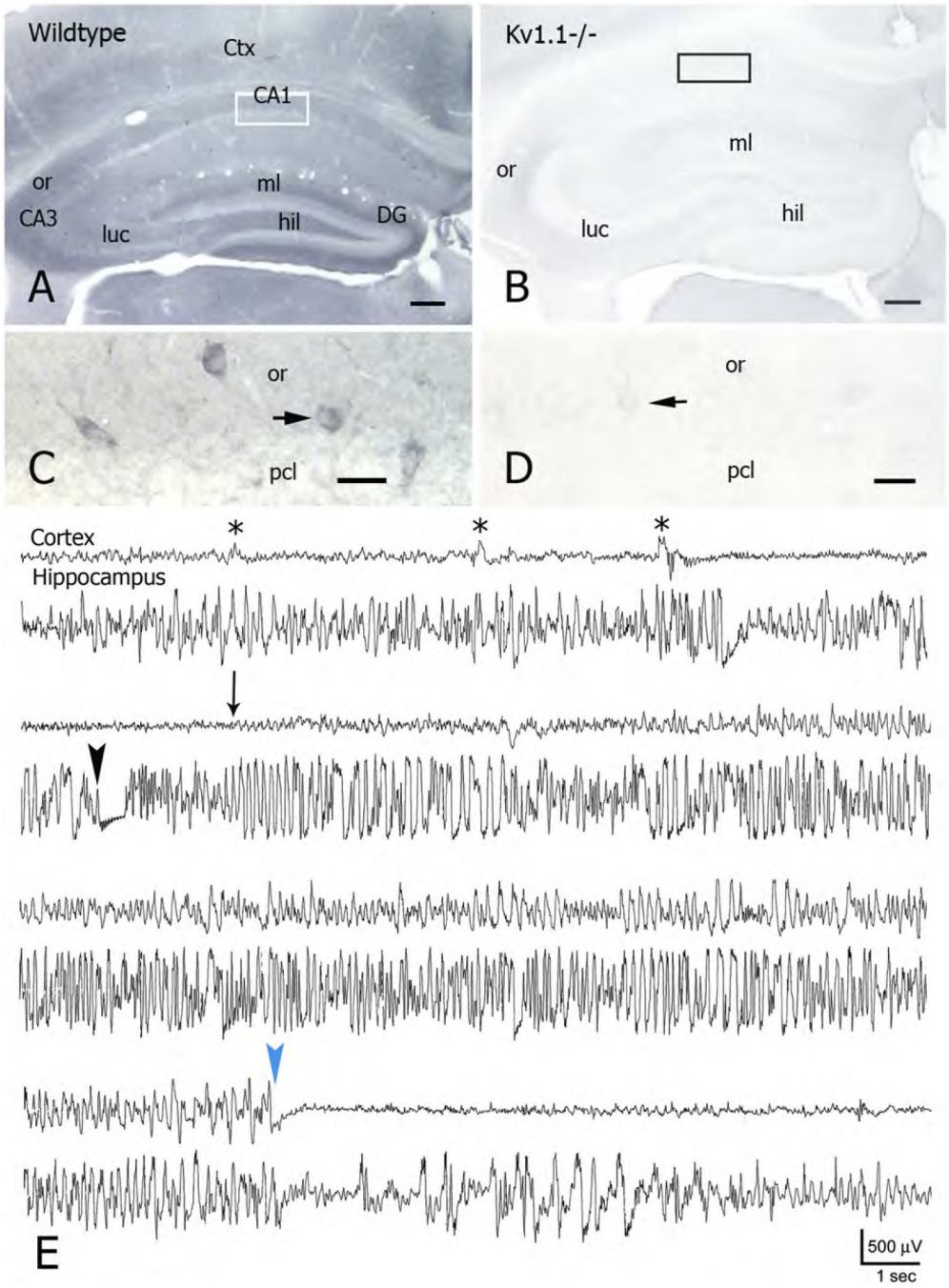

Figure 1. *Kcna1* gene deletion is associated with chronic, spontaneous seizures

A) Localization of Kcna1 immunoreactivity (IR) in a coronal section through the dorsal hippocampus of a 2 month-old wild-type mouse, showing particularly high IR in the dentate middle molecular layer (ml), hilus (hil), CA3 stratum lucidum (luc), and CA3 s.oriens (or). Abbrevations: CA1, CA3, hippocampal subfields; DG, dentate gyrus; Ctx, neocortex. B) Coronal section through the dorsal hippocampus of a 4 month-old Kv1.1$^{-/-}$ mouse. *Kcna1* gene deletion leads to a complete absence of Kcna1 IR (cf. IR in strata lucidum (luc), oriens (or) and moleculare (ml) in A).

C) Higher magnification of the indicated area in A, showing Kv1.1-positive neurons – presumed interneurons (e.g., arrow) in CA1 s.oriens (or) and at the border of the pyramidal cell layer (pcl).
D) Higher magnification of a comparable region from the Kv1.1 knockout hippocampus (indicated area in B). Faint profiles of presumed interneurons (e.g., at arrow) are Kcna1-immuno-negative.
E) Continuous EEG recording from neocortex (tope trace – Cortex) and hippocampus (bottom trace) of a Kv1.1 knock-out mouse. The top traces, before seizure onset, show occasaional interictal events, particularly evident in the surface recording (asterisks). An ictal episode began (second line) with EEG flattening in the hippocampal trace (black arrowhead); cortical reflection of seizure onset occurered somewhat later (thin arrow). In the hippocampal lead, the ictal episode began with fast spiking activity that increased in amplitude and progressed into a pattern associated with high amplitude spiking in the cortical lead. The high amplitude electrographic activity stopped abruptly (blue arrowhead) in both leads, with subsequent EEG depression with occasional low amplitude discharges. The electrical discharge was associated with a typical tonic-clonic behavioral seizure.
Scale bars: A and B: 200μm; C and D: 25μm..

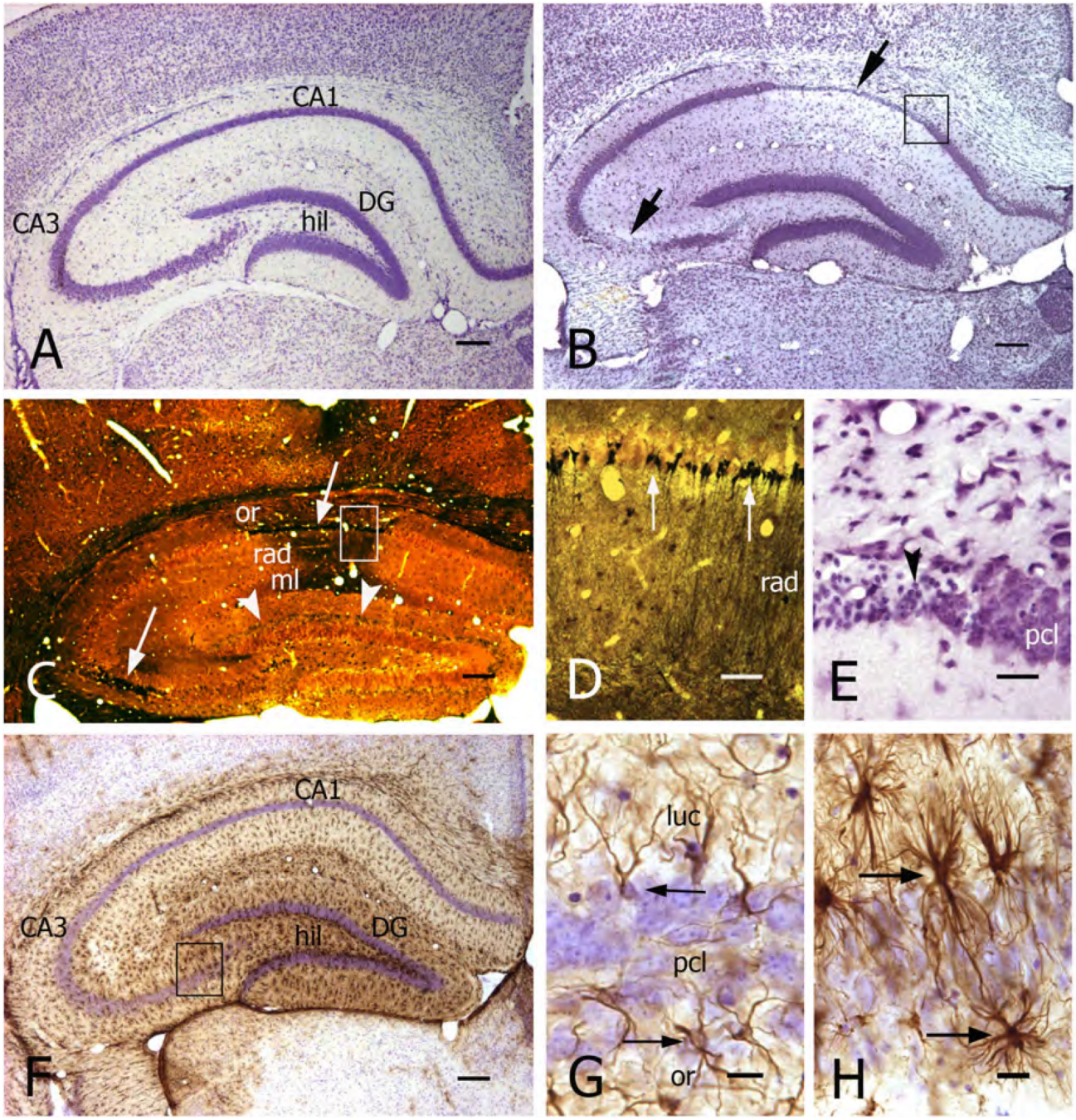

Figure 2. Chronic seizures in Kv1.1−/− mice are associated with severe pathohistological changes in hippocampus

A, B) Transverse sections of the hippocampus from a 10 week-old wild-type mouse (A) and an age-matched Kv1.1$^{-/-}$ mouse (B). Cresyl violet staining shows the normal histological pattern of hippocampal regions and laminae in A. In the knock-out (B), there was significant neuronal cell loss in CA1 and CA3b/c subfields (arrows).

C) Neuronal cell death and degeneration (particularly in CA1 and CA3 - white arrows) are shown in a Fink-Heimer-stained transverse hippocampal section from a 10 week-old Kv1.1$^{-/-}$ mouse. Note also terminal staining in the dentate inner molecular layer (arrowheads),

reflecting hilar mossy cell degeneration. Abbrevations: or, stratum oriens; rad, s.radiatum; ml, s.moleculare.

D) Higher magnification of the CA1 region (indicated area in C) showing degenerated CA1 pyramidal neurons within the pyramidal cell layer (black cell bodies) and terminal degeneration in strata radiatum (rad) and moleculare. Fink-Heimer staining.

E) Higher magnification of the indicated area in B, showing pyknotic pyramidal neurons (arrowhead) located in the CA1 pyramidal cell layer (pcl).

F) Transverse section of the hippocampus from a 5 month old Kv1.1$^{-/-}$ mouse, immunoreacted against GFAP. Note the high level of GFAP immunoreactivity (brown reaction product), particularly in the dentate gyrus (DG) and CA3c subfield. Cresyl violet counter-staining in F-H.

G, H) Photomicrographs comparing normal astrocytes (arrows in G) from CA3 of a wild-type mouse and reactive astrocytes (arrows in H, from boxed area in F) from a Kv1.1$^{-/-}$ mouse.

Scale bars: A-C, F, I, and J: 200μm; D and K: 50μm; E, G, and H: 20μm.

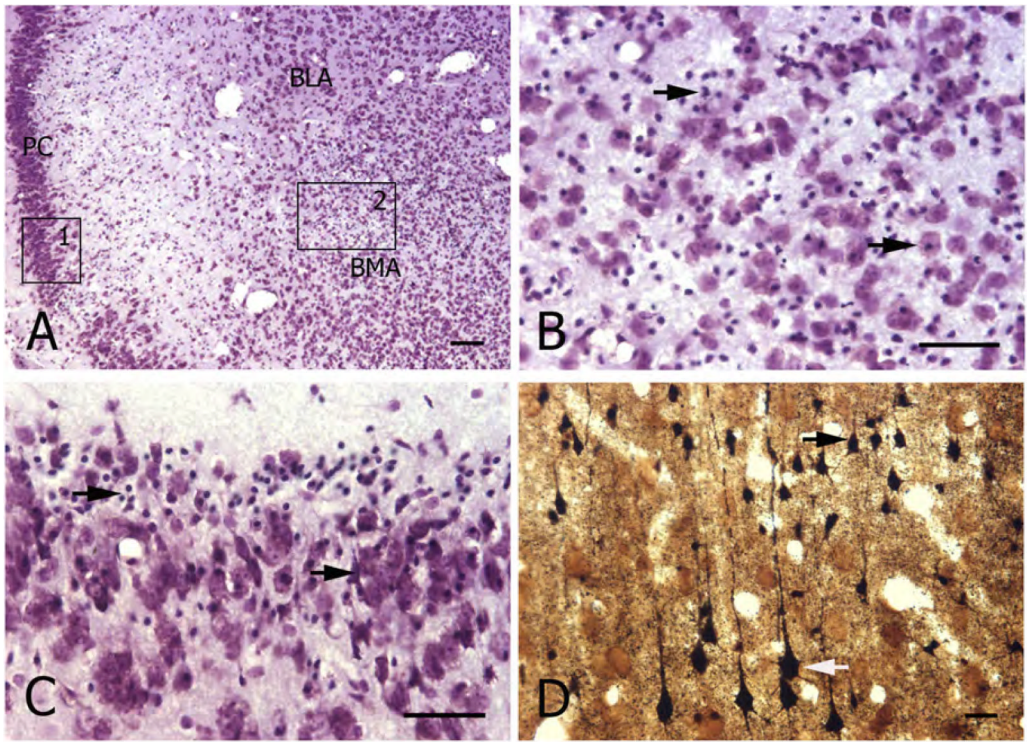

Figure 3. Chronic seizures in Kv1.1$^{-/-}$ mice are associated with pathological changes in multiple brain regions

A) Transverse sections through the brain (level of the rostral hippocampus) of a 10 week-old Kv1.1$^{-/-}$ mouse who experienced status epilepticus. Cresyl violet staining shows severe cell loss in piriform cortex (PC) and anterior basomedial amygdaloid nucleus (BMA). For comparison, note the relatively preserved neuronal architecture in the anterior basolateral amygdaloid nucleus (BLA).

B) Higher magnification of the amygdala (BMA) (indicated area 2 in A) showing neuronal cell loss and many pyknotic cells (arrows).

C) Higher magnificationof the piriform cortex (indicated area 1 in A) showing severe neuronal damage, including pyknotic cells (arrows).

D) Higher magnification of a Fink-Heimer stained transverse section from the parietal neocortex (same animal as in A-C above) showing degenerated neurons in layer II/III (black arrow) and degenerated layerV pyramidal neurons (white arrow).

Scale bars: A and D: 100μm; B and C: 50μm.

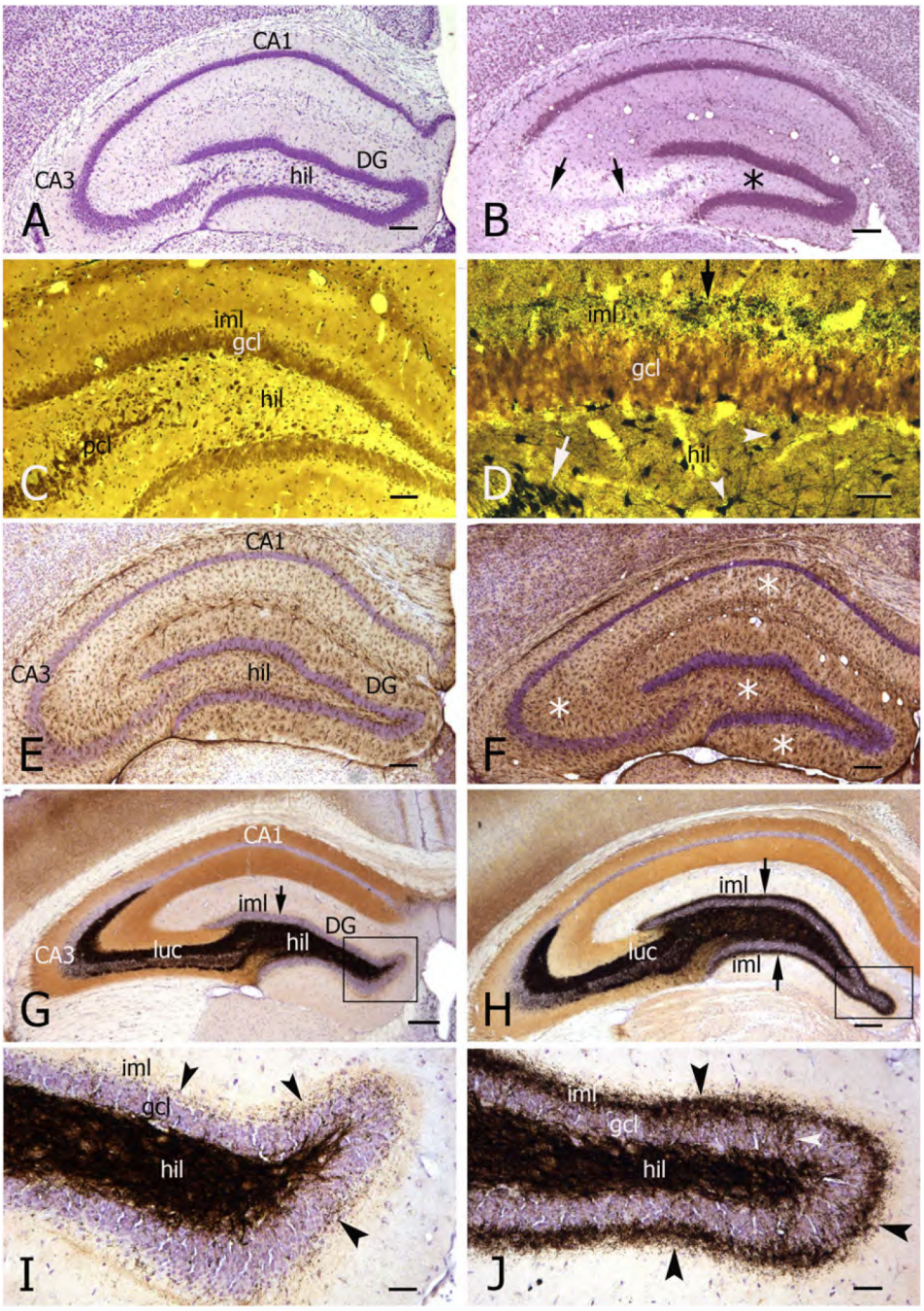

Figure 4. Variable pathologies in Kv1.1$^{-/-}$ mice reflect seizure severity

A) Transverse section of the hippocampus (cresyl violet-stained) from a 9 month-old Kv1.1$^{-/-}$ mouse. This animal showed only mild seizure activity, and histology revealed no obvious morphological damage in hippocampal subfields.

Abbrevations: DG, dentate gyrus; hil, dentate hilus.

B) In comparison, a transverse section from a 10 week-old Kv1.1$^{-/-}$ mouse experiencing status epilepticus shows severe neuronal cell loss in CA3b and c subfields (arrows) and dentate hilus (asterisk).

C) Fink-Heimer staining of the dentate gyrus reveals little degeneration within the dentate hilus (black puncta) of a 10 month-old Kv1.1$^{-/-}$ mouse with mild seizure history. Abbrevations: iml, inner molecular layer; gcl, granule cell layer; pcl, CA3 pyramidal cell layer.
D) Fink-Heimer staining of a transverse section of the dentate gyrus of a 10 week-old Kv1.1$^{-/-}$ status epilepticus mouse reveals degenerated CA3 pyramidal cells (white arrow) and hilar neurons (white arrowheads, indicating degenerated mossy cells and interneurons), as well as severe terminal degeneration within the inner molecular layer (iml; black arrow).
E, F) Transverse sections of the hippocampus of a 10 month old (E) and a 10 week-old (F) Kv1.1$^{-/-}$ mouse. GFAP-immunostaining (cresyl violet counterstaining) shows moderate gliosis in dentate gyrus (DG) and hippocampal CA3 subfield in E (mild seizure history) compared to the pattern of severe gliosis in the dentate gyrus and all hippocampal subfields (asterisks) in F (status epilepticus history).
G) Transverse section of the hippocampus from a 9 month-old wild-type mouse showing the normal staining pattern of Timm-positive mossy fiber boutons, localized to dentate hilus (hil) and CA3 strata lucidum (luc) and oriens. Cresyl violet counterstaining in G-J.
H) Timm staining of a transverse section from a 5 month-old Kv1.1$^{-/-}$ mouse, showing mossy fiber sprouting into the dentate inner molecular layer (iml; arrows) as well as into the granule cell layer and s.oriens.
I) Higher magnification of the dentate crest (indicated area in G) from a wildtype mouse, showing sparse Timm-stained mossy fiber boutons in the granule cell layer (gcl) and inner molecular layer (iml; arrowheads). Abbreviation: hil, dentate hilus.
J) Higher magnification of the dentate crest (indicated area in H) from a Kv1.1$^{-/-}$ mouse, showing intense mossy fiber sprouting into the granule cell layer (gcl; white arrowhead) and inner molecular layer (iml; black arrowheads).
Scale bars: A, B, and E-H: 200μm; C: 100μm; D, I and J: 50μm.

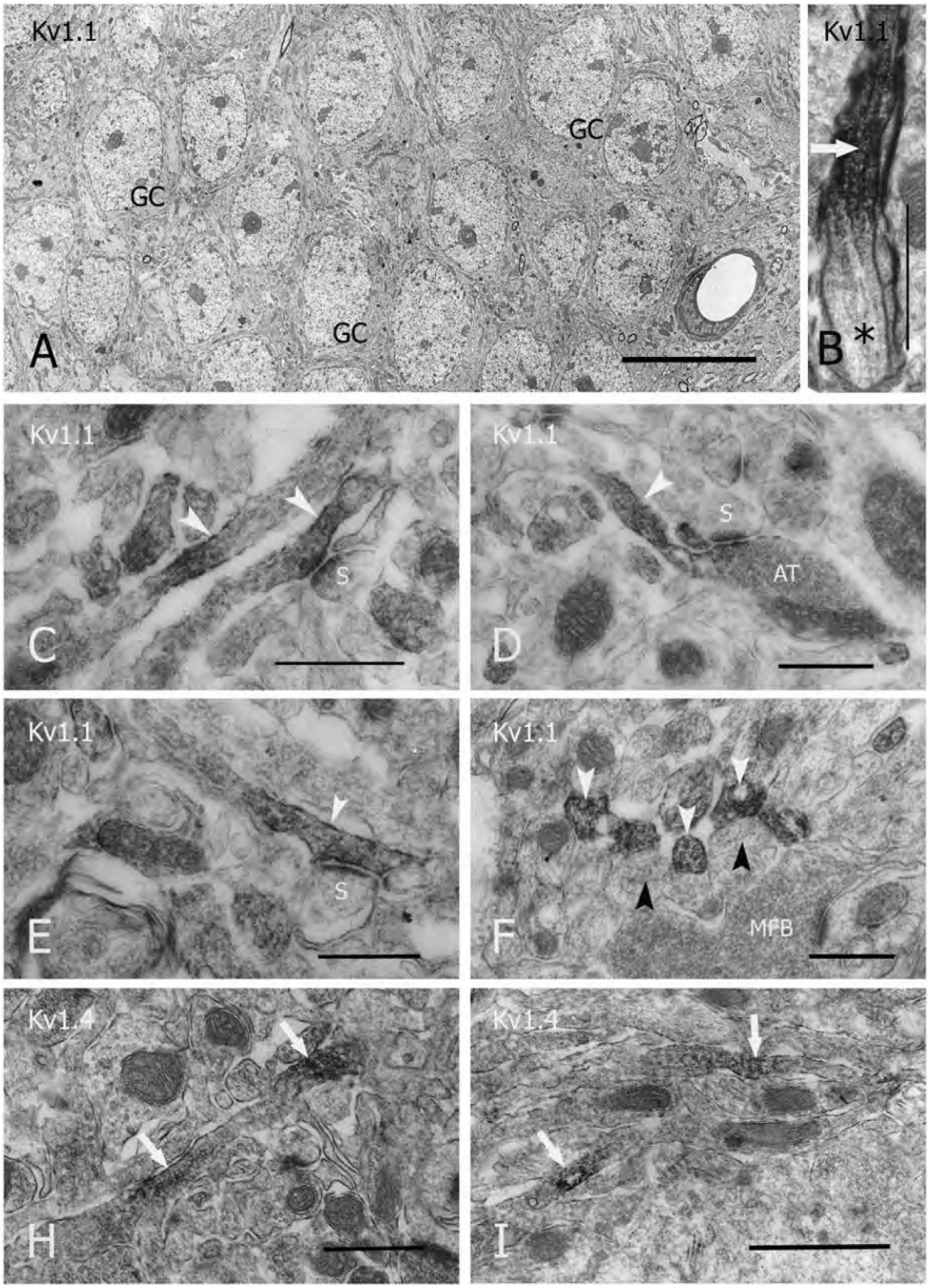

Figure 5. Ultrastructural localization of Kv1.1 channels in axons of the major hippocampal pathways in wild-type mice

A) Electron micrograph of the dentate granule cell layer from a 2 month-old mouse. The section was immunoreacted against Kcna1, and shows densely-packed granule cells (GC). Note the absence of Kcna1 IR within the granule cell bodies.

B) Electron micrograph of a myelinated axon in the hippocampal fimbria. Kcna1 IR is expressed at high level in the juxta-paranodal region (arrow) of the node of Ranvier localized to the axolemma and throughout the axoplasm - but not in the nodal or internodal regions (asterisk).

C, D) Electron micrographs of the dentate middle molecular layer from a 2 month-old mouse, showing Kv1.1 channel protein expressed in non-myelinated axons of the perforant pathway, localized to the extra-synaptic axonal membrane and axoplasm (arrowheads). Abbreviations: S, spine; AT, axonal terminal.

E) Electron micrograph of a Kcna1-positive non-myelinated axon (arrowhead) (within the dentate hilus) forming a synapse with a spine (S).

F) Electron micrograph of the CA3 s.lucidum, showing intense Kcna1 IR (white arrowheads) localized to the axonal membrane and within the axoplasm of fine mossy fiber axons. Note the absence of IR within the mossy fiber bouton (MFB). Some mossy fiber axons within the bundle are not labeled (black arrowheads).

H) Electron micrograph of the dentate middle molecular layer showing Kv1.4 channel IR (arrows) localized to the same set of fine axon profiles (perforant path fibers) immunolabeled by Kcna1 IR.

I) Electron micrograph of the CA3 s.lucidum showing Kv1.4 channel IR localized to fine axons (arrows) within the mossy fiber bundle in s.lucidum.

Scale bars: A: 10μm; I: 1μm; B-H: 500nm.

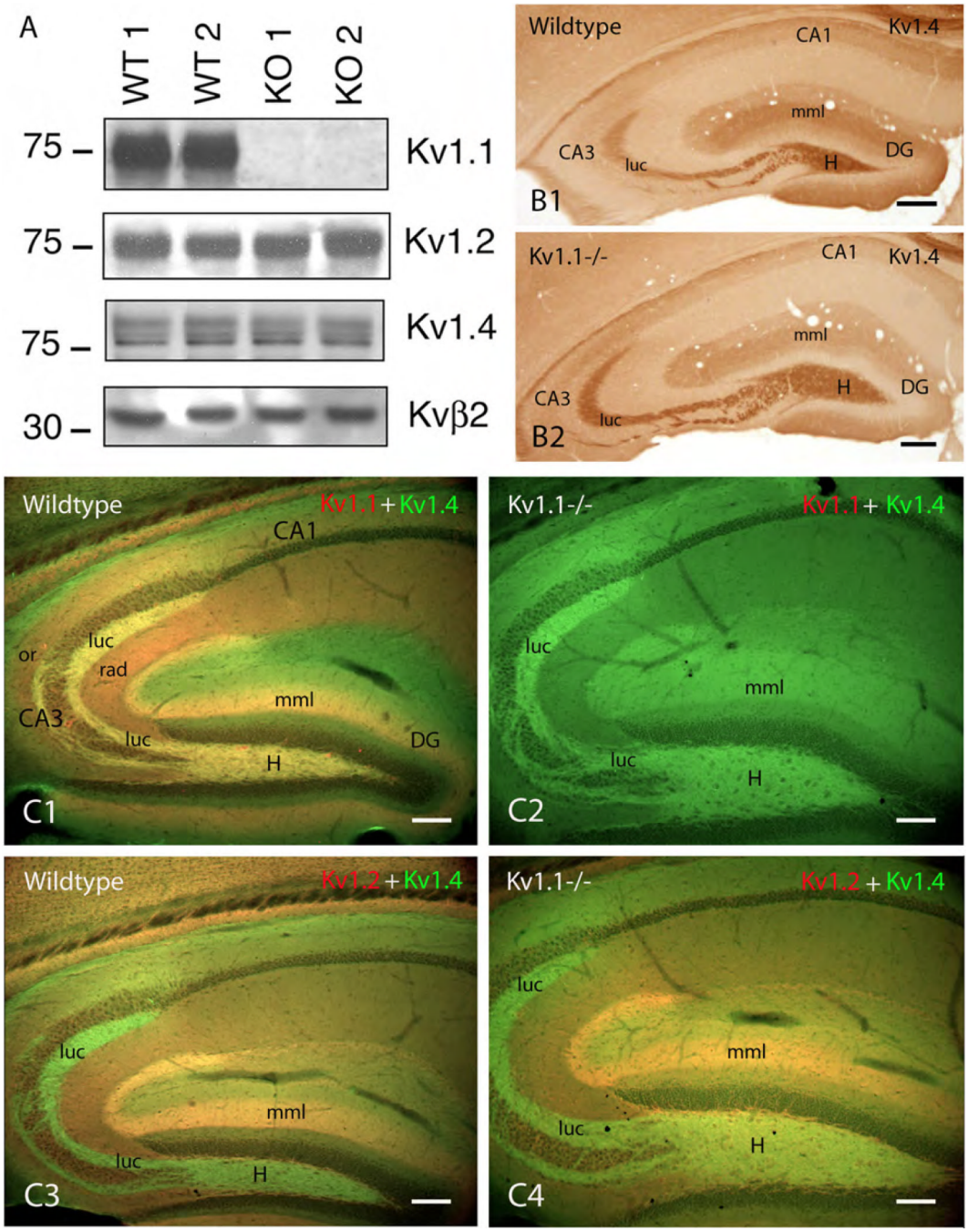

Figure 6. Effect of *Kcna1* gene deletion on Kv subunit and auxiliary subunit expression

A) Immunoblot of mouse brain membrane fractions were obtained from two different wild-type (WT1, WT2) and *Kcna1*-deficient (KO1, KO2) mice (two months old). Proteins (10 μg/lane) were extracted in SDS sample buffer, separated by SDS-PAGE, and analyzed for total Kv1.1 or different related Kv subunits (Kv1.2, Kv1.4, Kvβ2). Numbers at left refer to mobility of molecular weight standards (in kDa). None of the related proteins showed changes in $Kv1.1^{-/-}$ mice compared to controls. Similarly, there were no changes in other Kv (or auxiliary) proteins (e.g., Kv1.3, Kv2.1, Kv3.1 isoform β, Kv4.2, PSD-95, Slo) (not shown).

B) Kv1.4 channel protein immunocytochemistry in hippocampus of a wild-type and a Kv1.1 knock-out (Kv1.1−/−) mouse. In both animals, Kv1.4 is highly expressed in the hilus (H) and

s.lucidum (luc) of CA3, reflecting its localization in the mossy fiber axons. This channel subunit is also found in the middle molecular layer (mml) of the dentate gyrus (DG). Like Kv1.1, Kv1.4 is absent from granule cell and CA3 pyramidal cell somata. The ICC profile is consistent with the immunoblot data; there are no obvious changes in Kv1.4 density.

C) Double immunofluorescence staining of wild-type (left panels) and Kv1.1$^{-/-}$ (right panels) hippocampus. C1, 2. Double immunofluorescence staining for Kv1.1 (red) and Kv1.4 (green). Note loss of Kv1.1 staining in Kv1.1$^{-/-}$ hippocampus, and a lack of any dramatic change in the overall intensity or distribution of Kv1.4 staining.

C3,C4. Double immunofluorescence staining for Kv1.2 (red) and Kv1.4 (green). Note lack of any dramatic change in the overall intensity or distribution of Kv1.2 and Kv1.4 staining in wild-type versus Kv1.1$^{-/-}$ hippocampus (apparent decrease in Kv1.4 expression in the hilus of knock-out mice (lighter green in hilus in C4 compared to C3) is likely due to the increase hilar area in the knock-out, and the consequent “dilution” of Kv1.4-containing mossy fibers). Scale bars: B: 200 μm; C: 100 μm

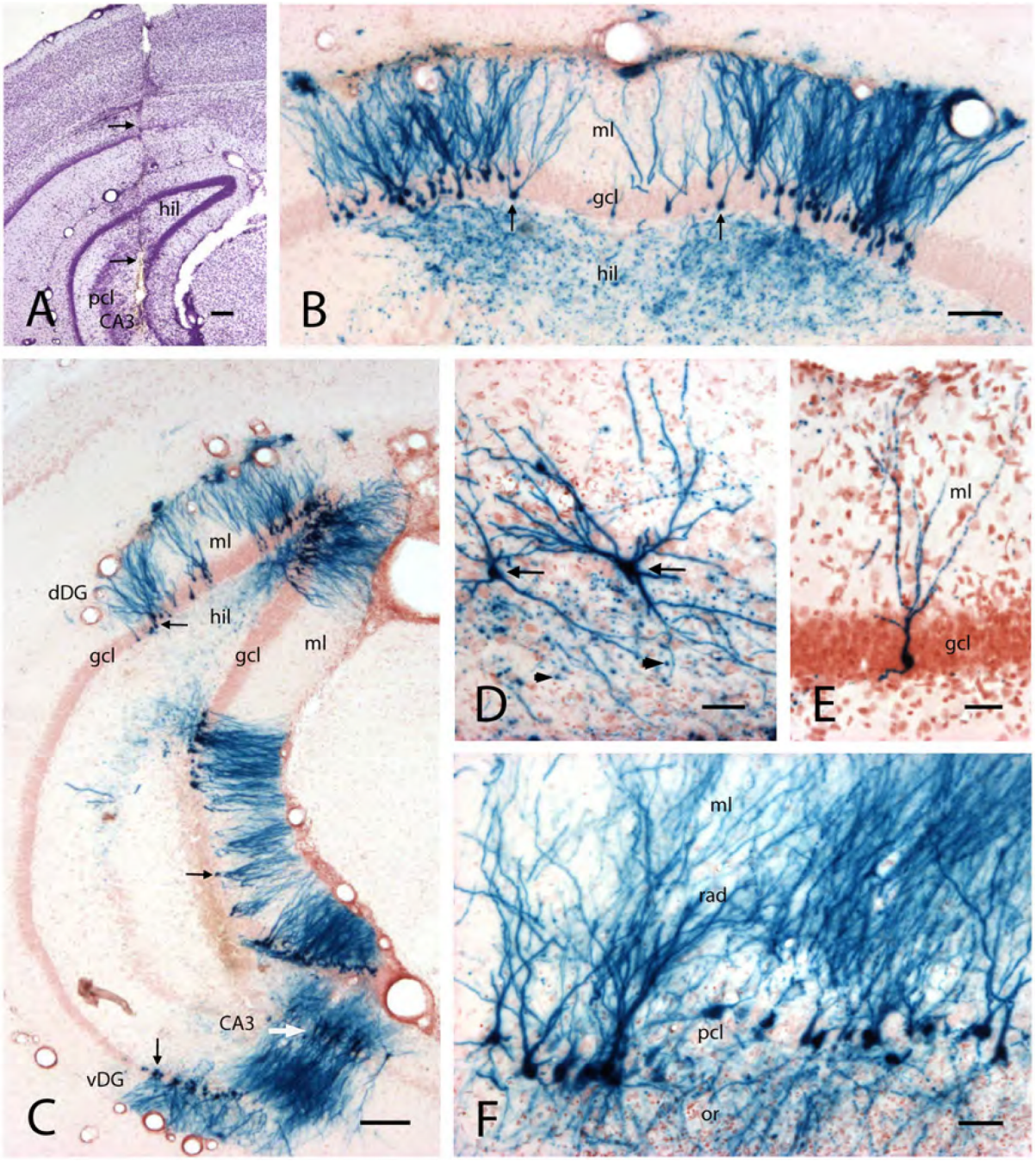

Figure 7. Hippocampal cell infection with HSVI viral vector containing genes for Kv1.1 channel protein and β-galactosidase

A) Transverse section from the caudal hippocampus, showing the track of a cannula (arrows) used for vector injection. The cannula tip is positioned within hilus (hil) and CA3 pyramidal cell layer (pcl).

B) Transverse section of the dentate gyrus in the dorsal hippocampus, showing β-gal in numerous granule cells (X-Gal histochemical staining, yielding blue cells). Note the complete staining of cell bodies (arrows) in the granule cell layer (gcl), dendrites in the molecular layer (ml), and mossy fiber axons and boutons in the hilus (hil).

C) Low power transverse section from the caudal hippocampus, showing X-Gal-stained granule cells (arrows) and CA3 pyramidal neurons (white arrow) in dorsal (dDG) and ventral (vDG) hippocampal/dentate gyrus regions. Abbrevations: hil, hilus; gcl, granule cell layer; ml, molecular layer.
D) Higher magnification of two representative X-Gal-stained CA3 neurons (arrows). Note the punctate staining around the cells, reflecting X-Gal-stained mossy fiber boutons (arrowheads).
E) Higher magnification of a representative X-Gal-stained granule cell.
F) Transverse section from the ventral hippocampus showing X-Gal-stained CA3 pyramidal neurons. Abbreviations: rad and ml, strata radiatum and moleculare; pcl, pyramidal cell layer; or, s.oriens.
Scale bars: A and C: 200μm; B: 100μm; D and F: 50μm; E: 20μm.

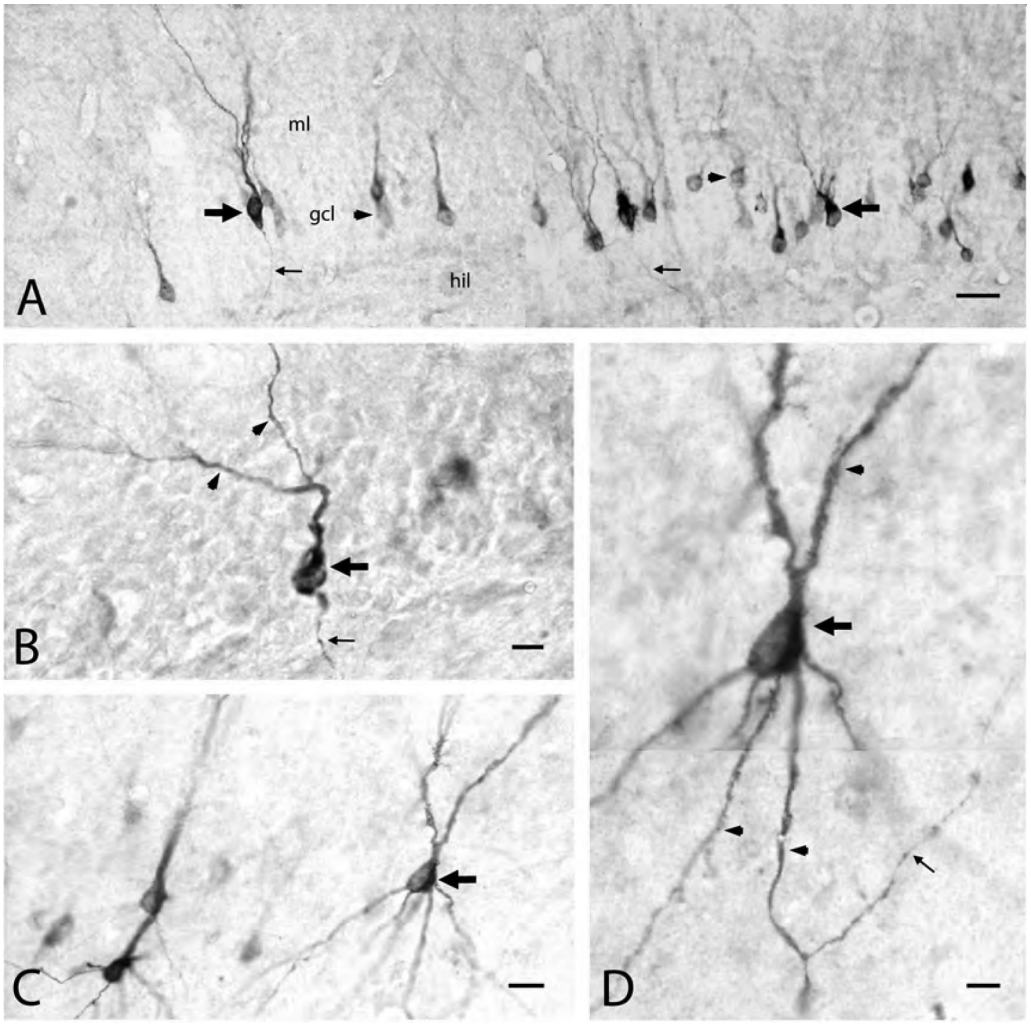

Figure 8. Immunocytochemical evidence of Kv1.1 channel α subunits in infected neurons of Kv1.1 knock-out mouse

A) Photomicrograph montage of the dentate granule cell layer (gcl) in a transverse section of the dorsal hippocampus immuno-reacted against Kcna1 anti-serum, from a 4 month-old Kv1.1-infected knock-out mouse. The animal was sacrificed 3 days post-infection. Immunocytochemistry shows numerous Kv1.1-positive GCs (large arrows), as well as many weakly-stained GCs (expressing low levels of Kv1.1 IR) (arrowheads). A few GC axons (i.e., mossy fibers) were also stained (small arrows).

B) Higher magnification of a Kv1.1-infected GC. Kv1.1 channel protein is highly expressed in soma (arrow), dendrites (arrowheads) and axon (small arrow). Background staining is likely an artifact (also seen in ICC of Kv1.1$^{-/-}$ mouse tissue).

C) Photomicrograph of the CA3 pyramidal cell layer showing several Kcna1-immuno-labeled neurons (arrow).

D) Two-dimensional reconstruction of one of the CA3 pyramidal neurons from C (same animal as shown in A) showing Kv1.1 channel expression in soma (arrow), dendrites (arrowheads), and axon (small arrow).

Scale bars: A and C: 20μm; B and D: 10μm.

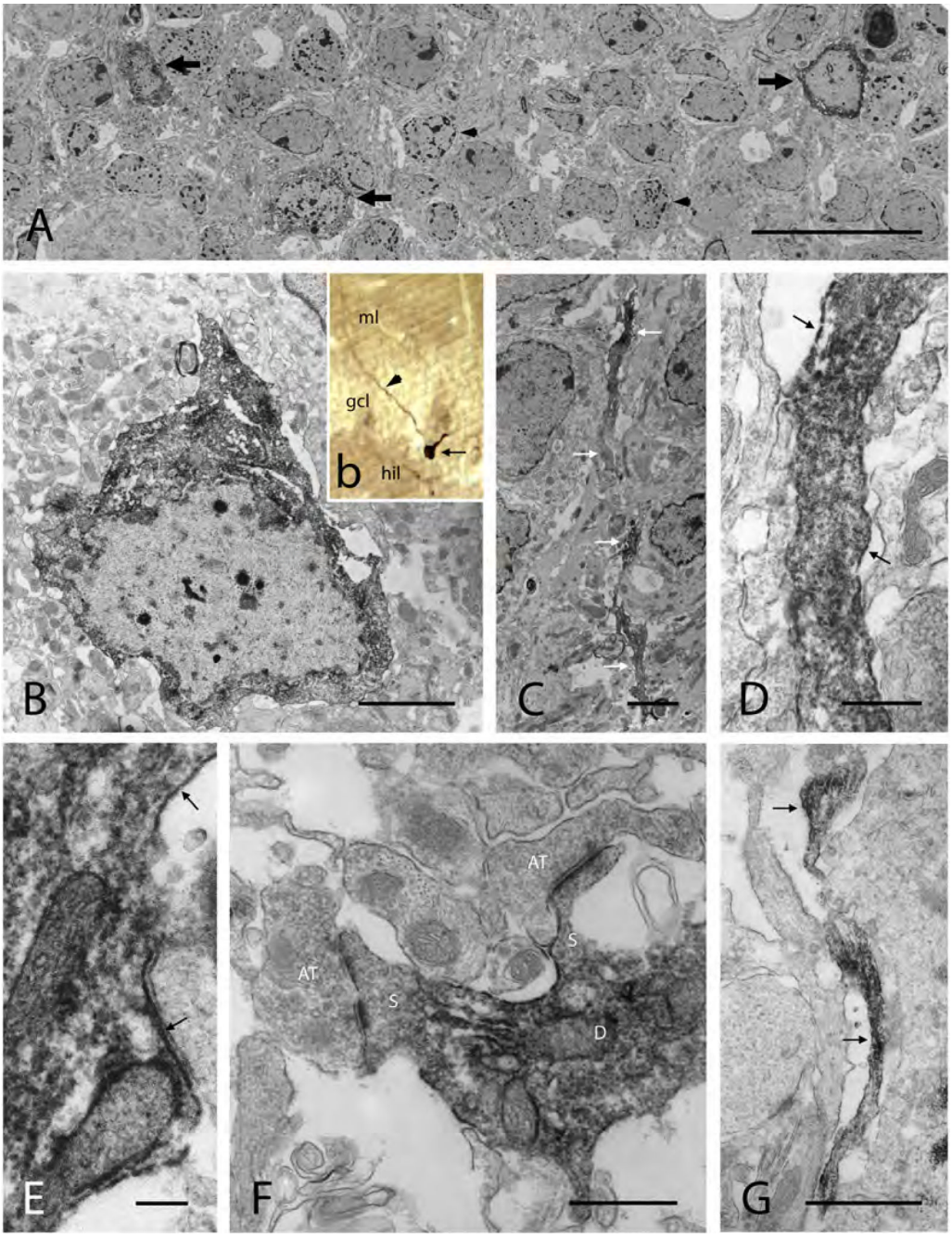

Figure 9. Ultrastructural localization of Kv1.1 channels in infected dentate granule cells of the Kv1.1 knock-out mouse

A) Low power electron micrograph of the dentate granule cell layer from a 4 month-old Kv1.1 knock-out mouse, showing three Kv1.1-infected granule cells (arrows) 4 days post infection. Note the pathological changes of nuclear chromatin in some of the GCs (arrowheads).

B) Electron micrograph of a Kv1.1-infected GC from a 9 month-old Kv1.1 knock-out mouse (4 days post infection), immuno-stained with an antibody against Kcna1. Inset b is a photomicrograph of this GC (arrow), which exhibits dendrites (arrowhead) within the granule cell layer (gcl) and molecular layer (ml) as well as a basal dendrite into the hilus (hil).

C) Electron micrograph of segments of a GC dendrite (white arrows) from the granule cell in B, showing Kv1.1 α subunit expression.
D) Higher magnification of a portion of the dendrite in C, showing intense Kcna1 IR on the dendritic membrane (arrows) and in the dendritic cytoplasm.
E) Higher magnification of the granule cell somatic cytoplasm (neuron in B), showing intense Kcna1 IR on the cell membrane (arrows) and also in the cytoplasm of the perikaryon.
F) Electron micrograph of a basal dendrite (C, D and inset b), exhibiting two spines (S) which form synapses with axonal terminals (AT). Note the Kcna1 IR on the spine membrane and in the dendritic cytoplasm.
G) Electron micrograph of a Kv1.1-positive axonal segment (mossy fiber; arrows) from an infected GC located within the granule cell layer.
Scale bars: A: 20μm; B and C: 2μm; G: 1μm; D and F: 500nm; E: 200nm.

Table 1

Quantitative assessment of seizure-induced neuronal damage and mossy fiber reorganization in the dentate gyrus of Kv1.1 knock-out and wild-type control mice.

Genotype	Average Number of Neurons (Mean ±S.E.M.)	Estimated Volume $\mu m^3 \times 10^6$ (Mean ±S.E.M.)	Average Density of Neurons per $\mu m^3 \times 10^6$ (Mean±S.E.M.)	Mossy Fiber Sprouting Score (Mean ±S.E.M)
Wildtype (WT) (n=4)	2798.64± 140.68	81.35±12.09	36.33±4.7	0
$Kv1.1^{-/-}$ - with mild/ moderate seizures (KO-Non-SE) (n=4)	2533.52±98.27	178.25±9.47	14.33±0.94	2.0±0.23
	WT vs. KO-Non-SE: No significant difference	*WT vs. KO-Non-SE: P<0.01*	*WT vs. KO-Non-SE: P<0.01*	
$Kv1.1^{-/-}$ - with status epilepticus (KO-SE) (n=4)	1273.61±110.42	165.56±19.13	8.12±1.5	2.86±0.15
	WT vs. KO-SE: P<0.001	*WT vs. KO-SE: P<0.01*	*WT vs. KO-SE: P<0.001*	
	KO-Non-SE vs. KO-SE: P<0.001	*KO-Non-SE vs. KO-SE: No significant difference*	*KO-Non-SE vs. KO-SE: No significant difference*	

Stereological cell counts of dentate hilar neurons, the measured/estimated hilar volumes, and the average neuron densities from three experimental animal groups. Data are expressed as mean ± S.E.M. Wildtype and KO-Non-SE mice were examined at 4.5 months of age. In the KO-SE group, age of sacrifice ranged from 10 weeks to 7 months. See Methods for a description of quantitative analysis and statistical testing. Mossy fiber sprouting score were based on the density of Timm staining within granule cell- and inner molecular layers (see Methods); only two KO-SE mice were evaluated because many of those animals died during the period required for reorganization. Given the semi-quantitative nature of mossy fiber sprouting scores, and the small sample sizes, no statistical testing was carried out.

Table 2

Summary of animals included in viral vector-mediated gene transfer study.

	Total Number of Mice	Numbers of Mice with Infection Rating		
		good	poor	none
Wildtype:				
lacZ alone	8	1 (4 mo / 4 dpi)	2 (3 mo/ 4 dpi)	5 (3.1 mo / 6dpi)
lacZ+Kcna1	5	3 (4 mo / 6.5 dpi)	2 (3 mo / 6 dpi)	0
Kv1.1−/−:				
lacZ alone	8	3 (4.5 mo / 3.7 dpi)	2 (3 mo / 5 dpi)	3 (3.3 mo / 6 dpi)
lacZ + kcna1	14	4 (4.8 mo /3.8 dpi)	5 (3.8 mo /4 dpi)	5 (2.1 mo / 6 dpi)

Vector efficacy was scored semi-quantitatively, based on the frequency and localization of β-gal-labeled hippocampal neurons, as follows: *good* - infection of many neurons in dentate gyrus and CA3 subfield; *poor* - sporadic labeling of single cells in dentate gyrus or CA3 subfield; *none* - no labeling of any neurons. Numbers in parenthesis indicate average age in months (mo) at time of vector infection, and average days post-infection (dpi) at the time of sacrifice and brain fixation (e.g., 3mo/4dpi).